A review of H-Darrieus wind turbine aerodynamic research

Longhuan Du[1], Grant Ingram[2] and Robert G. Dominy[3]

Abstract

The H-Darrieus vertical axis turbine is one of the most promising wind energy converters for locations where there are rapid variations of wind direction, such as in the built environment. The most challenging considerations when employing one of these usually small machines are to ensure that they self-start and to maintain and improve their efficiency. However, due to the turbine's rotation about a vertical axis the aerodynamics of the turbine are more complex than a comparable horizontal axis wind turbine and our knowledge and understanding of these turbines falls remains far from complete. This paper provides a detailed review of past and current studies of the H-Darrieus turbine from the perspective of design parameters including turbine solidity, blade profile, pitch angle, etc. and particular focus is put on the crucial challenge to design a turbine that will self-start. Moreover, this paper summarizes the main research approaches for studying the turbine in order to identify successes and promising areas for future study.

Key words: H-Darrieus wind turbine, design consideration, aerodynamic models, CFD, experimental approaches

Corresponding author: Longhuan Du (longhuan_du@163.com)
[1] College of Architecture and Environment, Sichuan University, Chengdu, China.
[2] Department of Engineering, Durham University, Durham, UK.
[3] Faculty of Engineering and Environment, Department of Mechanical & Construction Engineering, Northumbria University, Newcastle, UK.

Nomenclature

Parameter	Definition
A	Amplitude
Ar	Aspect ratio
c	Blade chord length
C_l	Lift coefficient
C_{nf}	Normal force
C_p	Power coefficient
D	Matrices for viscous resistance coefficients
n	Number of blade
R	Turbine radius
S	Blade Span
T	Torque
V	Upstream wind speed
α	Angle of attack
β	Blade pitch angle
θ	Azimuth angle
λ	Tip speed ratio
σ	Turbine solidity
ζ	Wavelength

Acronym	Definition
ADV	Acoustic doppler velocimeter
BEM	Blade Element Momentum
CFD	Computational Fluid Dynamics
DMST	Double Multiple Streamtube model
HAWT	Horizontal Axis Wind Turbine
IDDES	Improved Delayed Detached Eddy Simulation
LES	Large Eddy Simulation
MRV	Magnetic Resonance Velocimetry
NLF	Natural Laminar Flow
PIV	Particle Image Velocimetry
Re	Reynolds number
SPIV	Stereoscopic particle image Velocimetry
VAWT	Vertical Axis Wind Turbine
VTM	Vortex Transport Model

1. Introduction

As the world economy continues to grow, energy demand is likely to increase despite efforts increase the efficiency of energy use. The urgent need to meet this increasing demand and to reduce greenhouse gas emissions is being met, at least in part, by the development of large scale wind turbines, both onshore and offshore. Nevertheless, for some situations including urban centres and off-grid locations there is an argument for the development of local, decentralised production of electric power, to complement large scale electric power plants which are located in just a few specific, strategic locations. One of the most promising local production sources of clean electricity, for example in the built environment, is the small-scale wind turbine and, in particular, vertical axis machines that can tolerate large, rapid changes of wind direction. Although the small size of these turbines inevitably leads to a low power rating, in large numbers they can still contribute significantly to renewable energy production, improve building energy efficiency and make a considerable contribution to the future electricity generation mix.

1.1 Types of VAWTs

Wind turbines can be broadly classified into Horizontal Axis Wind Turbines (HAWTs) and Vertical Axis Wind Turbines (VAWTs) [1]. The most common example is the modern three-bladed HAWT shown in Figure 1(a), which generates torque, T, through aerodynamic lift. The designation horizontal axis means that the axis of rotation lies parallel to the incoming wind vector, V. Due to its high power coefficient and relatively light structural blade loading, this configuration nowadays dominates in the field of large-scale wind power generation both on land and offshore. Other iconic examples of HAWTs are the traditional Dutch windmill and the American-style wind pump shown in Figure 1(b) and Figure 1(c), respectively.

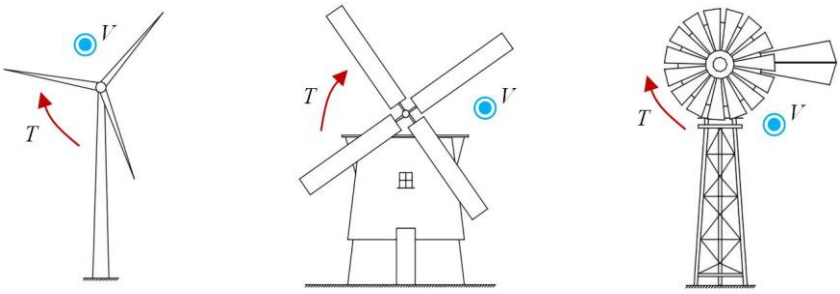

Figure 1 Typical Horizontal Axis Wind Turbine configurations [1]

The distinctive characteristic of the VAWT is that the axis lies perpendicular to the direction of the wind instead of parallel [2]. This allows the device to capture energy from any wind direction. The most well-known VAWT is the lift-driven Darrieus machine, which is named after the French aeronautical engineer Georges Jean Marie Darrieus (1888-1979) as shown in Figure 2(a) and Figure 2(b). This wind turbine consists of a set of vertically orientated blades/aerofoils connected to a rotating shaft, and is characterised by its Troposkien (C-shape) or H-shape rotor blades. It is normally built with two or three blades and previous studies (e.g.[3, 4]) have demonstrated that the lift-driven Darrieus machine can produce a higher maximum power coefficient comparing with the alternative, drag-driven Savonius VAWT [2] as shown in Figure 2(c).

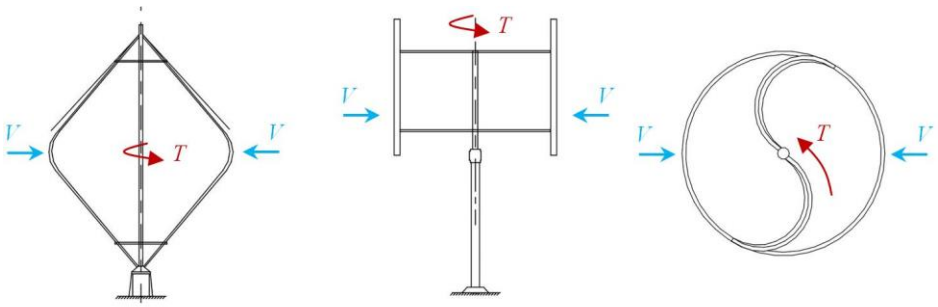

Figure 2 Typical Vertical Axis Wind Turbine configurations [1]

1.2 Advantages and disadvantages of H-Darrieus VAWTs compared to HAWTs

Although it is widely believed that HAWTs are more efficient than VAWTs of equal scale, VAWTs have attracted increasing research interest in recent times due to some inherent advantages. The advantages of the H-Darrieus VAWT, especially when used in high turbulence and low wind speed environments, are briefly as follows [5-7]:

- The turbine is insensitive to wind direction and consequently it does not require a yaw mechanism[8].
- Optimal blades can be simple in design, with a constant section along the span without twist or taper. This is a consequence of having a constant blade radius over their entire span so all sections of the blade operate at the same tip speed ratio and relative wind direction. It could be argued that the ground boundary layer might be considered through small changes in blade profile or even radius with height above the ground but for small VAWTs the variation of ground effect is small.
- Aerodynamic noise from the turbines is lower due to the constant blade radius which avoids the extreme tip speed of a horizontal turbine of comparable rating.
- Turbine performance is much less affected by varying flow direction and high as experienced, for example, in the urban environment.
- The heavy transmission system, generator and control system can easily be situated at ground level allowing easy installation, operation and maintenance. A further benefit is that without the constraint of a HAWT nacelle the transmission and generator can be configured to minimise rotational inertia with direct benefit to unaided starting.
- Studies show that turbines can be installed much closer to each other [9, 10] since the turbines are able to gain from the vortices shed by the turbines located upwind[11]. Therefore the site power density could be considerably higher than for the configurations used presently.

However, H-Darrieus VAWTs also present some disadvantages when compared to HAWTs:

- Complex turbine aerodynamics due to the constantly changing azimuth angle and blade angle of attack.
- Low starting torque and possible complete failure to self-start even under no-load conditions [12].
- Torque and power fluctuation during each revolution as the blades rotate (reduced by increasing the blade number).
- High bending moment due to centrifugal acceleration, which presents a design challenge especially for small turbines [13].

1.3 Aim of this paper

Although the Troposkien configuration has structural advantages, the simplicity and higher specific power of the H-Darrieus design make it popular for small-scale applications. The configuration remains the focus of most recent and current VAWT research, hence its selection as the focus of this review. In recent years VAWT research has accelerated dramatically both through experimentation and numerical simulation but our understanding of some fundamental aspects of their performance remains incomplete. Experimental measurements have been performed but

their scope has remained almost entirely restricted to steady state, overall power extraction and torque characteristics with little attention to the more difficult measurement and interpretation of the underlying flow physics. Explanations of the turbine's performance have therefore been based mostly on simulation studies because of the difficulty of applying traditional measurement methods such as thermal anemometry and pressure sensors to the rotating turbine. That situation is now changing with the more widespread use of experimental techniques such as particle image velocimetry (PIV) alongside developments in numerical simulation as researchers have access to the computing power required to simulate the time-accurate flow physics. The research community is now in a position to resolve some of the outstanding debates surrounding these turbines and, most particularly, that surrounding their capability to self-start without external assistance.

This paper aims to summarize the state of our knowledge and understanding of the aerodynamic characteristics of the H-Darrieus wind turbine with a particular focus on the crucial challenge to design a turbine that will self-start.

2. H-Darrieus turbine design considerations

2.1 Turbine critical self-starting behaviour

VAWT research has focused mostly on small machines operating in or near the urban environment where their insensitivity to the rapidly changing wind direction and atmospheric gusting makes them better suited than most alternatives.

A review of previous research into the operation of vertical-axis turbines reveals inconsistency in the use of terminology and in particular the definition of self-starting. Ebert and Wood [14] defined the starting process as having been completed when significant power extraction commences, and Kirke [13] adopted a similar definition in which a turbine was considered to be self-starting only if it could accelerate from rest to the point where it started to produce useful output. In both cases, the definition of the terms 'significant power' and 'useful output' are themselves imprecise. Others (e.g. Lunt[15]) adopted a more specific definition by which a turbine was deemed to have started if the rotor had accelerated from rest to a steady speed that exceeded the wind speed arguing that for this to occur significant lift must be produced during the rotational cycle. Although more precise, this definition also has its limitations. In particular, there is evidence that reaching the point at which the blades begin to produce lift over a significant part of a revolution does not guarantee that the machine will continue to accelerate. More recently, the turbine was deemed to be self-starting only if the turbine could accelerate from rest to the tip speed ratio where thrust was continuously generated over the Darrieus flight path according to Worasinchai et al.[16], which was similar to the definition used by Du et al. [5].

Turbine starting behaviour was investigated experimentally by Hill et al.[17]. In their experimental tests, a three-bladed H-Darrieus machine equipped with NACA0018 blades was tested in a $2\ m^2$ open-return wind tunnel. The turbine rotor was held stationary until the wind tunnel's speed had stabilized at its predetermined value. The release of the rotor triggered the start of the data capture process. Each trial began from a random starting position and it was found the angular position had no discernible effect on behaviour, which was consistent with Dominy et al.[18] who concluded that a three-bladed rotor would self-start irrespective of its starting position. Their wind tunnel testing of this three-bladed turbine with no generator load demonstrated a repeatable starting characteristic thus confirming that a H-Darrieus turbine using symmetrical aerofoils could reliably self-start in a steady airflow.

Hill el al. [17] identified four stages of the staring process (see Figure 3). The first stage was an approximately linear acceleration from rest to a tip speed ratio close to one, followed by a plateau stage where the increase of turbine rotational speed became very slow which some refer to as the 'dead band' (e.g.[19-22]). Some researchers, notably Ebert and Wood [14], hypothesised that a turbine could not accelerate through this 'dead band' because it corresponds to a zone of negative torque. However, observations in the laboratory and in the field provide clear evidence that a simple turbine can drive through the dead zone (see Figure 3). If the tip speed ratio (λ) can gradually increase to about $\lambda = 1.5$ the rotor then can accelerate rapidly to its maximum speed of $\lambda \approx 3$ (stage 3) and enter its steady operating stage (stage 4).

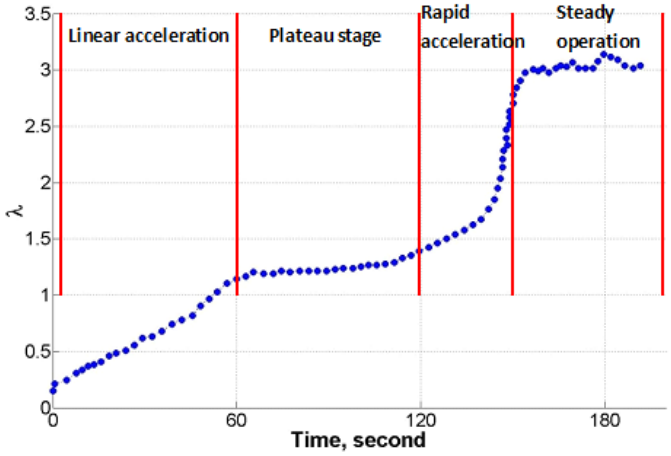

Figure 3 Measured H-Darrieus turbine starting behaviour from Hill et al.[17].

To better understand the starting process, Du et al.[5] performed a detailed experimental study of the influence of selected design parameters on a model H-Darrieus wind turbine. Time-accurate data were recorded from wind tunnel tests which clearly revealed the influence of design parameters including blade profile, solidity and blade number on the machine's performance through the complete starting period. Arab et al.[23] and Untaroiu et al.[24] investigated the turbine self-starting using numerical models. Although their predicted $C_p \sim \lambda$ curve followed the experimental results, the turbine plateau stage was not clearly captured by the numerical model resulting in an over-prediction of turbine self-starting time. Batista et al.[25], Rossetti and Pavesi [22], Dumitrescu et al.[26], Asr et al.[27], Douak et al.[28], Sengupta et al.[29] and Singh et al.[30] also studied the effect of solidity, blade profile, pitched angle etc. on the turbine starting behaviour. A summary of experimental data which can be used to validate transient numerical and analytical models when starting is presented in Table 1.

Configuration	Du et al.[5]	Hill et al.[17]	Dumitrescu et al.[26]
Number of blades	3	3	3
Aerofoil	NACA0021, DU06W200	NACA0018	NACA0018
Chord length (m)	0.1	0.083	0.08
Blade span (m)	0.7	0.6	0.3
Turbine radius (m)	$0.3, 0.37, 0.45$	0.375	0.25
Solidity	$1.0, 0.81, 0.67$	0.664	0.96
Aspect ratio	7	7.229	3.75
Wind speed (m/s)	6 and 7	6	11.7
Self-start or not	Yes	Yes	Yes
Reynolds number ($\times 10^4$)*	4 ~ 4.7	3.4	6.3
*The Reynolds number is calculated based on the upstream wind speed in present study			

Table 1 Some available sources of time-resolved experimental data for different turbine configurations.

2.2 Turbine solidity

Solidity has a strong influence on turbine performance affecting power coefficient C_p variation with tip speed ratio λ, the turbine's maximum efficiency and its self-starting capability. The solidity of an H-Darrieus wind turbine is a measure of ratio of blade area to turbine swept area and is defined as

$\sigma = \frac{nc}{R}$ although it should be noted that there is an alternative definition of $\sigma = \frac{nc}{2R}$, which is adopted by some authors. Templin [31] recognised that increasing the solidity would result in greater blockage of the flow, causing a reduction of the incoming flow velocity and local changes of flow direction as more flow has to pass around the device. These blockage-induced direction changes result in lower angles of attack in the upstream half of the rotor allowing the flow to remain unstalled at lower tip speed ratios. A direct consequence is that the peak power coefficient occurs at a lower value of λ, but the continued reduction of angle of attack as λ increases means that the aerodynamic torque generated is less than that for a lower solidity rotor at high λ. Moreover, the efficiency of high solidity machines dropped away quickly either side of the optimum λ while the $C_p - \lambda$ curve was flatter for low solidity machines as identified by previous studies (e.g. [13, 32-36]). Howell et al.[37] pointed out the importance of solidity in determining the rotational velocity at which the turbine reached its maximum performance coefficient and Castelli et al.[38] studied the effect of blade number, demonstrating that the peak power coefficient fell with the increase of rotor solidity as a consequence of a larger number of blades attaining maximum power coefficient for lower angular speeds, but with an efficiency penalty. Recently, Subramanian et al.[39], Rezaeiha et al. [40], Li et al.[41], and Sagharichi et al.[42] also investigated the solidity effect on the turbine performance. The above studies demonstrated that turbine peak power coefficient decreased with the increase of solidity and a high solidity was preferred when turbine initial self-starting torque was required.

Low solidity turbines enjoy a relatively large power output for a large range of λ since the $C_p - \lambda$ curve is flatter making them less sensitive to sudden changes in wind speed (Figure 4), but there is a conflicting argument that a turbine's solidity should be increased to improve its self-starting performance (e.g. [43-46]) and thus potentially resulting in improved overall efficiency(e.g. [5, 30, 47]).

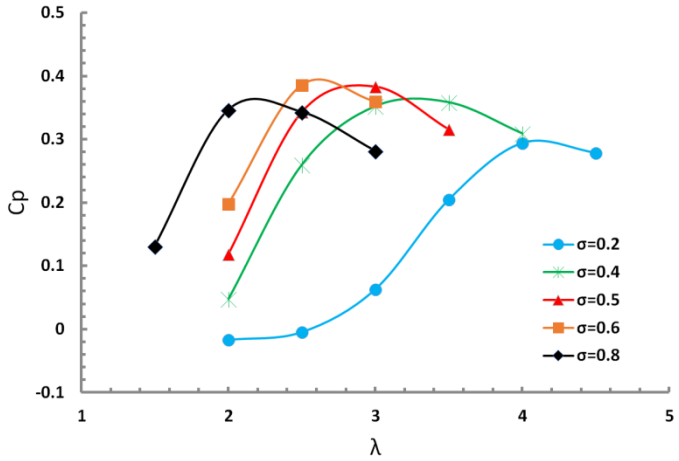

Figure 4 Effect of solidities on fixed pitch VAWT power curve performance [42]

2.3 Number of blades

As noted by Kirke [13], the power produced by a wind turbine depends primarily on the wind velocity and the swept area, not on the blade area. Therefore a single blade machine is potentially as efficient as turbines with two or three blades, in terms of the percentage of kinetic energy that can be extracted and converted to shaft power but at low λ a forward torque cannot be produced by a single blade at the majority of azimuth angles, resulting in an inability to self-start.

The number of blades, not only relates to solidity but also to the variation in loading on the turbine structure as the turbine rotates. Varying loads are an inherent part of VAWT operation and fatigue was a serious issue with early VAWTs [48] which should be considered in the design stage. According to the studies performed by Consul et al.[33], Goselin et al.[34] and Mcintosh et al.[49], the variation of torque was shown to be significantly reduced with three or four blades rather than two. Moreover, Sabaeifard et al.'s study [50] also demonstrated a three-bladed H-Darrieus turbine was preferred.

From the perspective of self-starting, it has been shown that although two-bladed turbines have the potential to self-start that capability does not extend to all possible starting positions which could prove to be problematic for commercial turbines [18]. Three-bladed turbines were reported to be self-starting (e.g. [5, 17, 18]) irrespective of their starting position with careful rotor and blade design and are therefore preferred.

2.4 Blade profile

In the early studies of H-Darrieus turbines, symmetrical NACA00xx profiles, in particular NACA0012, NACA0015 and NACA0018, were widely adopted. These profiles were well understood and data were available covering a wide range of conditions, which made aerodynamic design and theoretical power prediction relatively easy. However it was soon recognised that these aerofoils, which were developed for aviation, might not be the best for VAWT application and that specially designed blades, such as laminar flow aerofoils, cambered profiles or increased thickness profiles could improve turbine performance.

A set of aerofoils was developed by Sandia researchers [51, 52], known as natural laminar flow (NLF) aerofoils, with the objective of improving the turbine performance. However, a study conducted by Masson et al. [53] demonstrated that limited gains could be get by using he NLF blades comparing with the symmetrical NACA00xx profiles, especially at large wind speeds. Keeping a symmetrical profile but increasing the blade thickness had also been proposed since a thicker blade profile might be more beneficial to the VAWT structural engineer trying to create a blade with good bending resistance, which would make it possible to have longer blade spans and/or higher rotational speeds. Angell et al.[54] had shown that sections up to approximately 21% thickness may be used with no loss in performance at Reynolds number (Re) of the order of 1.5×10^6. More recently, Islam et al.[55], Du et al.[20], and Mcintosh[49] also identified the potential advantages of thicker blades including improved starting performance and lower noise at Re from $\sim 10^4$ to $\sim 10^5$.

Kirke [13] suggested that cambered aerofoils such as those used on relatively low Reynolds number aircraft may perform better than traditional symmetric aerofoils. According to his study, some cambered airfoils was far superior to that of symmetrical ones in the upwind region (positive incidence) and more than offset the loss of performance in the downwind region (negative incidence), resulting in improved overall performance and self-starting capability. More recent studies [29, 55-58] also featured analysis on cambered aerofoils suggesting improved the turbine performance at Re of $10^4 \sim 10^5$. Mohamed [59] carried out a study using a 2-D CFD model with 20 different blade profiles (symmetric and asymmetric) in order to maximize the output torque coefficient and the output power coefficient. Based on his study, it was demonstrated that the cambered S-1046 airfoil increased the power output by 26.83% compared to the standard symmetric NACA airfoils. Meanwhile turbine noise were also studied by Mohamed [60] by using various blades. It was found S-1046 was the better airfoil from the noise point of view due to less aerodynamic nose generation and increasing the tip speed ratio and solidity would increase turbine noise.

Recently, Claessens [61] proposed a new aerofoil designated as DU06W200. This new aerofoil was designed specifically for VAWT application having 20% thickness with 0.8% camber. According to that study the DU06W200 demonstrated a 5% increase of peak power output compared with the NACA0018. Moreover the whole curve ($C_p - \lambda$) was shifted left (see Figure 5) which indicated that the new proposed aerofoil could generate more torque (power) at low tip speed ratios, increasing the turbine self-starting capability. Studies performed by Ikonwa et al.[62] also indicated DU06W200 blade possessed a high starting torque and could be an ideal blade to eliminate the problem of self-starting. However, the experimental measurement performed by Du et al.[5] at Re of 4.7×10^4 demonstrated the NACA0021 has similar performance and self-starting behaviour but with simpler design without any camber.

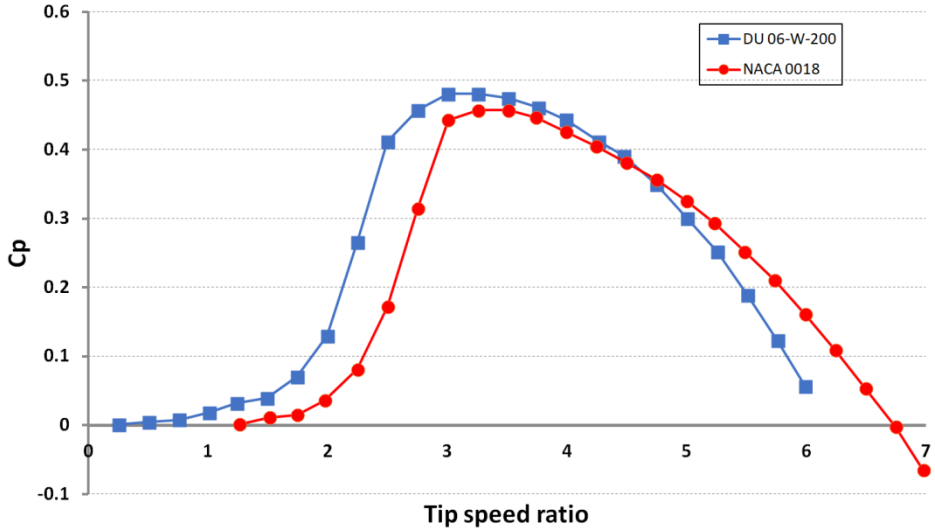

Figure 5 Turbine power coefficient with DU06W200 profile compared with NACA0018 profile [61]

More recently, Du et al.[5] proposed to use of bio-inspired blades for H-Darrieus wind turbine to extend the unstalled incidence range. This idea came from the humpback whale (see Figure 6(a)), which is exceptional among the large baleen whales in its ability to undertake aquabatic manoeuvres to catch prey [63]. Modifications could be made by creating a sinusoidal tubercle configuration at the blade leading edge with proper wavelength, ζ, and amplitude, A, (see Figure 6(b)). Moreover, previous static wind tunnel measurements [64-66] found that by creating tubercles around the blade leading edge, sudden stall could be successfully replaced by a more gradual stall behaviour and the tubercles significantly increased the blade lift performance in the post-stall regime but at the expense of slightly degraded lift performance in the pre-stall regime. According to previous static wind tunnel measurements of different tubercle configurations[66], the validation test for the optimum combination of $A = 2$ mm and $\zeta = 7.5$ mm for NACA0021 was performed by Du et al.[5] on an H-Darrieus wind turbine at Reynolds number of 4.7×10^4. It was demonstrated experimentally by Du et al.[5] that this bio-inspired blade could significantly increase the turbine self-starting capability at the expense of slightly lower peak power output, which was consistent with the numerical studies performed by Wang and Zhuang[67] and Wang et al.[68]. These blades are very promising candidates for the future application in the low wind environment.

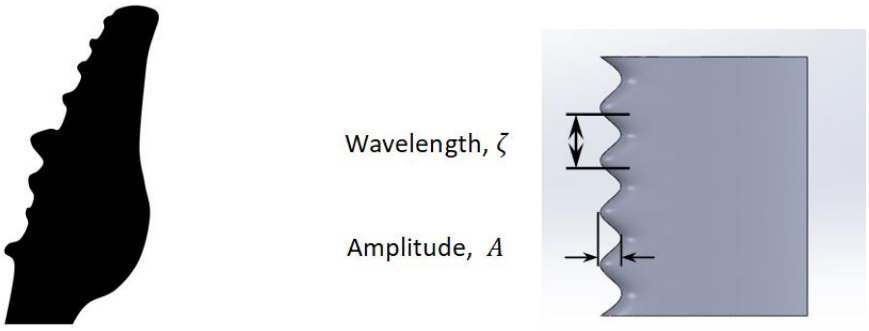

(a) (b)

Figure 6 (a) Schematic drawing of the humpback whale flipper with large rounded tubercles along the leading edge and (b) Definition of tubercle wavelength, ζ, and amplitude, A [5].

Researchers continue to investigate blade profiles for H-Darrieus application (e.g. [69, 70]), but the results remain inconclusive and sometimes conflicting. The traditional symmetrical NACA series with large thickness still presents a simple but effective choice of blade geometry achieving a good compromise between good starting performance and adequate peak power operation.

2.5 Curvature effect

As first pointed out by Migliore et al.[71], the aerodynamic characteristics of an aerofoil differ for curvilinear and rectilinear flow. A symmetrical aerofoil moving in a curved path has the same aerodynamic characteristics as a cambered aerofoil moving in a rectilinear flow field with a virtual angle of incidence as shown in Figure 7. Migliore et al.[71] illustrated that the flow curvature effects became more pronounced at large c/R ratio. The blade performance will be modified due to the curvature effects and it must be considered when translating conventional aerofoil data for VAWT applications, as confirmed by a study performed by Rainbird et al.[72].

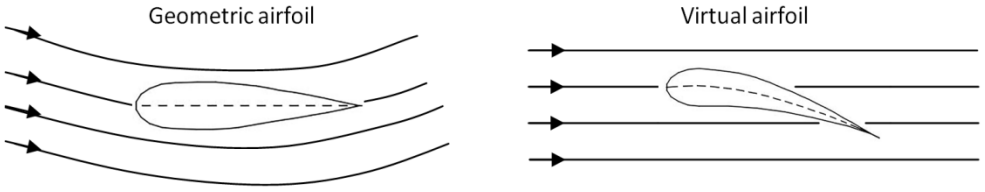

Figure 7 Schematic drawing of curvature effects for symmetric blades moving in a curvilinear flow [71]

Due to the orientation of the virtual camber, an additional normal force acts toward the centre of rotation and the normal force is increased during the upstream pass and decreased during the downstream pass. Sharpe's[73] analysis provided an expression for the contribution to normal force as $C_{nf} = 0.25(\frac{dC_l}{d\alpha})\frac{c}{R}\lambda$. Early theoretical models (e.g.[74-76]) still produced surprisingly good results without taking the curvature into consideration. But in part this might be because the effects of flow curvature only become significant at high λ as pointed out by Soraghan et al.[77]. Nevertheless studies conducted by Goude [78] clearly demonstrated that analytical models with curvature correction predicted turbine performance that better matches experiments and the experimental measurements performed by Du et al.[5, 79] further demonstrated that the virtual camber effect increased with the increase of λ and that this 'virtual camber' correction factor must be implemented in analytical models as proposed by Bianchini et al.[80]. As proposed by Balduzzi et al.[81], at the design stage the curved flowpath experienced by the blade should be taken into consideration to compensate the curvature effects.

2.6 Pitch control strategy

Many of the disadvantages of H-Darrieus turbines relative to other types stem from the fact that there is cyclical variation in the angle of attack on the blades as the turbine rotates. As a result optimal loading cannot be sustained for all azimuth angles, leading to inherently low aerodynamic efficiency. This is further exacerbated as the blades depart from their optimal lift to drag ratio at most azimuth angles. Additionally, pulsating lift causes significant ripples in the torque and power generated. It has been argued that the ability to pitch the blades as they move around the path of rotation would address these disadvantages to some extent by sustaining optimal or near-optimal angles of attack for most azimuth angles [82]. The usual definition of blade pitch (β) is shown in Figure 8. Blade nose out is negative pitch ($-\beta$) and nose in is positive pitch (β).

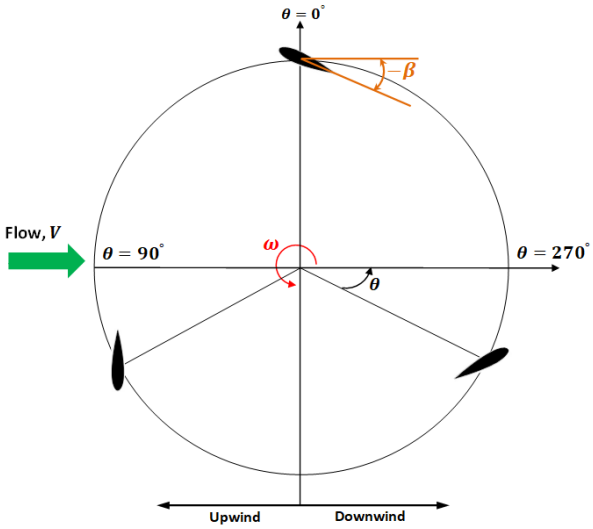

Figure 8 Definition of blade pitch angle [5]

2.6.1 Active pitch control

Active pitching would improve turbine control. Many of the significant improvements in wind turbine performance (especially HAWTs) over the past three decades have been due to the move towards pitch control. Pitch regulation has not only improved energy capture, but also achieved secondary objectives with the most important being the ability to alleviate transient structural loads[83]. The optimization of blade pitch similarly offers benefits in terms of HAWT performance but the application strategy is very different since the primary requirement of blade pitching for a VAWT is to minimize the cyclical changes of blade lift caused by rotation whereas for HAWTs it is to optimize for atmospheric wind variation. Many authors (e.g.[58, 84-86]) have applied analytical or numerical models to investigate the effect of active pitch and to determine optimal pitch strategies for H-Darrieus devices. For example, Chen et al.[87], using a simple sinusoidal pitch variation demonstrated that the power efficiency was improved significantly (up to 38%) and that the ripple factor of the power output was correspondingly. Numerical studies conducted by Sagharichi et al.[42] demonstrated the variable pitch strategy could lead to an improved turbine power production, which should be applied especially at low λ and Abdalrahman et al.[88] proposed that the application of active pitch control using an intelligent neural network would provide an appropriate technique.

In practice, active pitch control could be implemented for individual blades. Based on the individual aerodynamic load balance on blades, a formulation of the pitch angle is determined for each blade. The self-acting variable pitch mechanism uses aerodynamic forces to actuate self-acting devices and works by creating pitching moment about the blade pivot [43]. Furthermore, blade pitch angle could also be controlled actively by gears or cam actuator devices as used in the pinson cycloturbine [86, 89]. This method is also named collective blade pitch mechanism since the change of pitch angle is same for all blades

The problems of dynamic stall on an H-Darrieus turbine could be completely avoided if the blades could have their pitch varied with azimuth angle to achieve the optimal angle of attack around the entire revolution. However, active pitch mechanisms have been regularly dismissed as too complicated and expensive in the context of relatively small turbines [90]. Moreover, it is difficult to design an active pitch mechanism/strategy which works well in the whole operating range of the VAWT under different wind conditions. Therefore, a promising compromise is to adopt a pre-set, non-zero fixed pitch angle, which will be discussed in the following section.

2.6.2 Fixed pitch control

With a negative pitch angle ($-\beta$) as shown in Figure 8, the angle of attack in the upstream half of the rotor will be reduced but increased in the downstream half of the rotor. Therefore fixing a pitch angle in this way can be thought of

as a translation of the angle of attack curve up or down by exactly the pre-set pitch angle as shown in Figure 9. The blade dynamic stall is delayed since the angles of attack are reduced in the upstream half of the rotor which leads to the blade producing torque for a greater portion of the revolution [91].

According to Rezeaiha et al.[92], a 6.6% increase of C_p was achieved by setting the blades at $\beta = -2^{\circ}$ compared to $\beta = 0^{\circ}$ and the numerical studies conducted by Somoano et al.[21], Douak et al.[28], Parra-Santos et al.[93], Gosselin et al.[34] and Asr et al.[27] illustrated that a negative pitch angle could increase the turbine peak C_p providing confirmation of this effect. Du et al.[5] further demonstrated that a small negative pitch angle could also improve the turbine self-starting capability and reduce the turbine starting time.

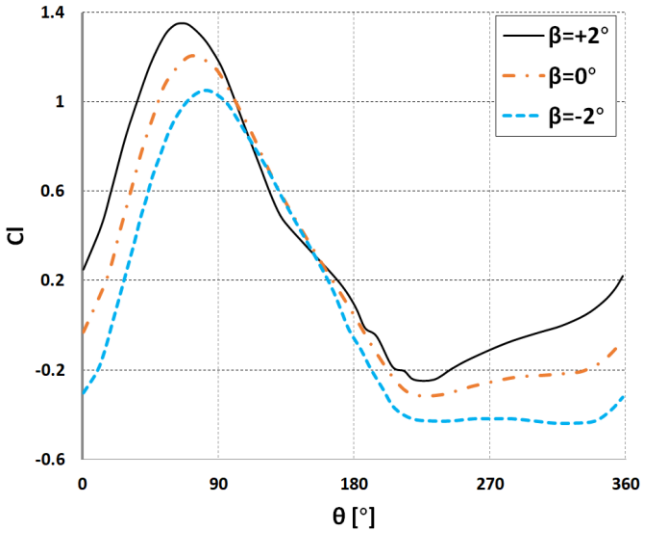

Figure 9 Blade lift coefficient versus azimuth angle for pitch angle of $\beta = -2^{\circ}$, $\beta = 0^{\circ}$ and $\beta = +2^{\circ}$ [92].

2.7 Surface roughness

A turbine's blade surface roughness will be expected to increase during its lifetime through erosion or contamination, potentially affecting the machine's performance and these effects need to be quantified and understood in the context of the vertical axis turbine.

Tests conducted by Ashwill [94] showed a noticeable effect when the blades became contaminated with 'bug reside'. In their tests, the turbine rotated at a constant speed of 28 RPM while the wind speed was varied and the 'bug reside' blades underperformed the clean blades by up to 7% at high λ. However, at low λ the results were reversed with the 'bug reside' blades showing clear performance gains. Howell et al.[37] investigated experimentally the influence of blade surface roughness on the turbine power output using blades manufactured from high-density foam to provide the largest scales of roughness which were later smoothed by finishing the surface with fine-grade glass paper. Their measurements (shown in Figure 10) illustrated that at low wind speeds the turbine with the rougher surface increased performance significantly. In contrast, the turbine performance was decreased with the rough surface blades at high wind speeds which might be due to the increased skin drag [37]. Li et al.[95] investigated how attachments (clay) impacted on the operational performance finding that the attachments reduced the power coefficient and the power reduction rate increased as the weight of the attachment and wind speed increased. Du et al.[5] developed research in the field to encompass transient turbine behaviour through the investigation of turbine self-starting behaviour under two different blade surface roughnesses. According to their measurements, the blades with rough surfaces only improved the turbine performance at low λ (starting period) when the turbine solidity was large ($\sigma > 0.67$). Under these circumstances, it was hypothesised that the better performance was due to the rough blades tending towards an earlier laminar to turbulent boundary layer transition resulting in the flow becoming more likely to remain attached and consequently blade stall was delayed [5, 37]. Nevertheless, it was discovered that when the turbine solidity was low, the blades with smooth surfaces were able to accelerate the turbine much faster than with rough blades leading to an overall better starting and steady state performance. The suggested explanation was that the flow blockage was reduced at low

turbine solidity resulting in the blade stalling over a larger portion of the revolution. Thus the benefit from the delayed stall of a rough surface became limited and could not make up for the loss from the increased skin friction drag. In addition, Priegue and Stoesser [96] found the blade roughness affected negatively the turbine performance and the rougher the blade, the poorer the performance of the turbine. The negative effect of blade roughness was much more significant at high blade Reynolds number according to their study. However, their experimental measurements were only performed at relatively large λ.

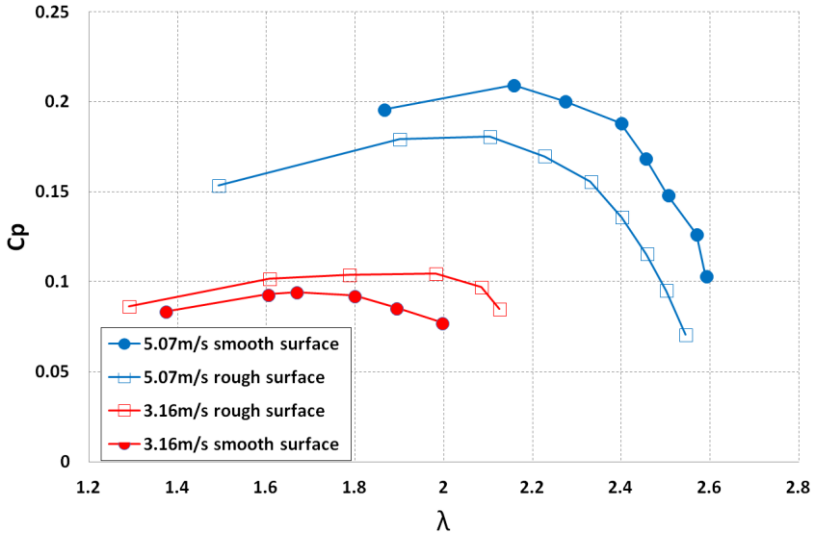

Figure 10 Turbine power output at different wind speed for smooth and rough blade surfaces [37]

2.8 Reynolds number effects

Approaches utilising data from blades/aerofoils designed for aviation applications have limited potential for studying small-scale VAWTs since the data are usually measured at Reynolds numbers that are relevant for aerospace (Re = $10^6 \sim 10^7$) but which lie far above those of a small VAWT where the Reynolds number experienced by the blade is typically one or two order of magnitude lower [97]. For an H-Darrieus wind turbine, the Reynolds number is based on blade chord length and the relative velocity but since the relative wind changes cyclically in both velocity and direction the Reynolds number is far from constant even at a steady tip speed ratio. For example, a blade moving away from the wind at a tip speed ratio of one results in an instantaneous Reynolds number of zero whereas 180 degrees later, when moving into the wind the relative velocity rises to twice the wind speed. The Reynolds effects are not only limited to the power extraction efficiency but also on the lifespan of the machine.

Meana-Fernandez et al.[98] suggested that when the turbine size was confirmed at the design stage, a cut-in and cut-out wind speed should be chosen to maximise the fatigue life. Numerical studies performed by Gosselin et al.[34] demonstrated that the Reynolds number only affected the blade performance significantly in the upwind region where most power is generated, while in the downwind region no significant difference was found. Amstrong et al.[99], noted that when the Reynolds number was greater than $500{,}000$, the power production of the turbine was essentially independent of Reynolds number while Zanforlin and Deluca[100] supported that conclusion by showing that the Reynolds number does not appreciably affected the blade pressure distribution under those conditions.

The effect of Reynolds number on the turbine power output was investigated numerically and experimentally by Sheldahl et al.[101]. With a constant turbine rotational speed and varying free steam velocity their measurements demonstrated that the Reynolds number change has very limited effect at low tip speed ratios but that the peak power coefficient and the power coefficient at high λ increase with the increase in Reynolds number, which was consistent with the results from Danao et al.[102]. However, the experimental measurements performed by Du et al.[5] at two freestream wind speeds of $V = 6m/s$ ($\mathrm{Re} = 40{,}000$) and $V = 7m/s$ ($\mathrm{Re} = 47{,}000$) clearly demonstrated that the small Reynolds number change had a significant effect on the turbine self-starting capability and starting time.

Therefore, as suggested by Meana-Fernandez et al.[98], when the wind speed was known for certain application, the Reynolds analysis would help to discard certain turbine sizes at the design stage.

3. H-Darrieus turbine research approaches

In the past two decades, there have been three main investigative tools [103]:

- Analytical aerodynamic models
- Computational Fluid Dynamics (CFD)
- Experimental measurements

A brief review for each method is provided here but the reader should refer to the specialised publications for in-depth information on these complex and rapidly developing approaches to the solution of fluid dynamics problems.

3.1 Analytical aerodynamic models

The most applied aerodynamic models for studying H-Darrieus VAWTs can be broadly classified into three categories which are (1) Momentum models, (2) Vortex models, and (3) Cascade models.

3.1.1 Momentum model

- **Single Streamtube model**

The first attempt at using momentum theory to study VAWT was the Single Streamtube model proposed by Templin [31]. This was a simple prediction method for the calculation of the performance characteristics of a Darrieus VAWT in which the induced velocity (rotor axial flow velocity) was assumed to be constant through the turbine which is represented by an actuator disc within which the momentum equation is solved by equating the streamwise drag with the change in axial momentum (Figure 11).

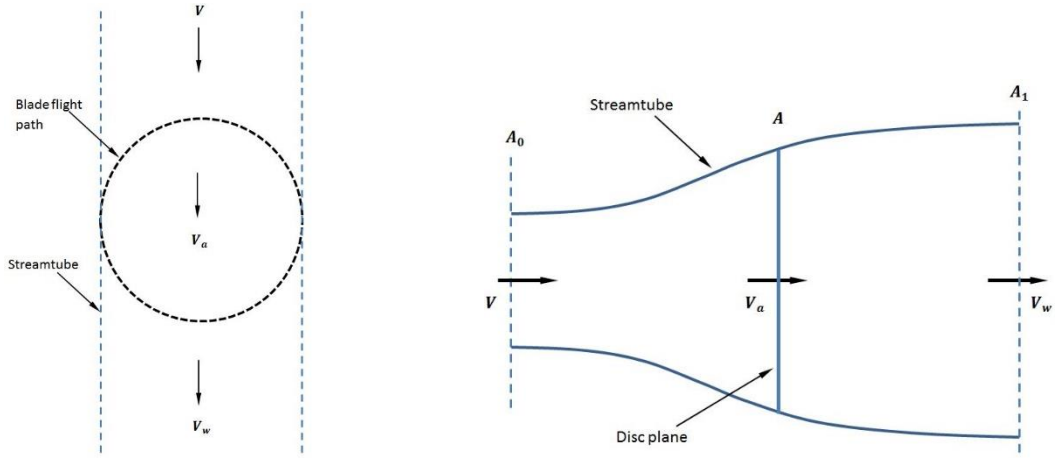

(a) (b)

Figure 11 Schematic drawing of (a) single streamtube model and (b) actuator disc theory [5]

This model can predict the overall performance of a lightly loaded wind turbine but it always predicts higher power than the experimental results. It does not consider the wind velocity variation across the rotor (wind shear) and the model is based on the several assumptions such as no frictional drag, non-rotating wake, homogenous and incompressible fluid and etc.[104].

- **Multiple Streamtube model**

Wilson and Lissaman [3] improved the single streamtube model by dividing the rotor into a series of adjacent, aerodynamically independent parallel streamtubes as shown in Figure 12. The blade element and momentum theories were then employed for each streamtube. By taking the blade drag into consideration, Strickland [105] further improved the model and Muraca et al.[106] developed the model by including the effects of aerofoil geometry, support struts, blade aspect ratio, turbine solidity and blade interference. In a further development Sharpe[107] incorporated the effects of Reynolds number into his BEM model. Read and Sharp [108] proposed another multiple streamtube model which replaced the parallel streamtube by an expanding streamtube concept. Recently, Tai et al. [109] and Roh et al.[45] also investigated the H-Darrieus performance based on the multiple streamtube model.

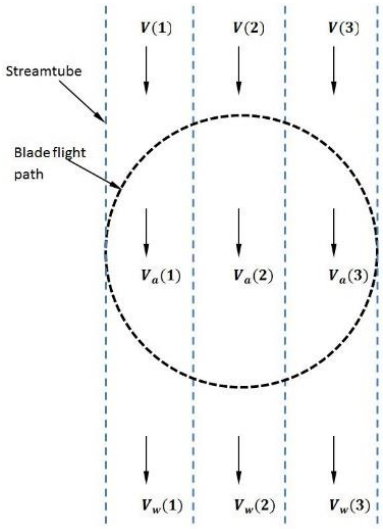

Figure 12 Schematic drawing of Multiple Streamtube model [5]

- **Double Multiple Streamtube model (DMST)**

The concept of using two actuator discs in tandem for a Darrieus wind turbine was originally suggested by Lapin [110] using a development of the method of Paraschivoiu [111] who introduced the Double Multiple Streamtube model, which incorporated the differences in the rotation of the upwind and downwind sections through the division of each streamtube into two halves, upwind and downwind respectively, as shown in Figure 13(a). Calculations were performed separately for each half cycle (Figure 13(b)). With an additional actuator disc at the downwind section signifying a secondary induction factor, the turbine interacted with the wind twice so the predictions were more accurate relative to the original Multiple Streamtube approach. The study performed by Paraschivoiu et al. [112] demonstrated the significant influence of secondary effects including the blade geometry, rotating tower and the presence of struts, especially at high tip speed ratios. Later, Paraschivoiu and Delclaux [74] improved this DMST model by considering the induced velocity variation as a function of the azimuth angle for each streamtube. Although the DMST provides better correlation between the calculated and experimental results, this model over-predicts power output for a high solidity turbine and there appears to be a convergence problem especially in the downstream side and at the higher tip speed ratios [104].

Further developments include a broad evaluation of the aerodynamic design and economic aspects of H-Darrieus turbines by Saeidi et al.[113] and Svorcan et al.[114] using the DMST model and annual energy yield was investigated by Bianchini et al.[115] using VARDAR (an improved DMST model with variable interference factors [8, 56]). The gyroscopic effects on a two-bladed H-Darrieus wind turbine on a floating structure was also investigated by Blusseau and Patel [116] using DMST.

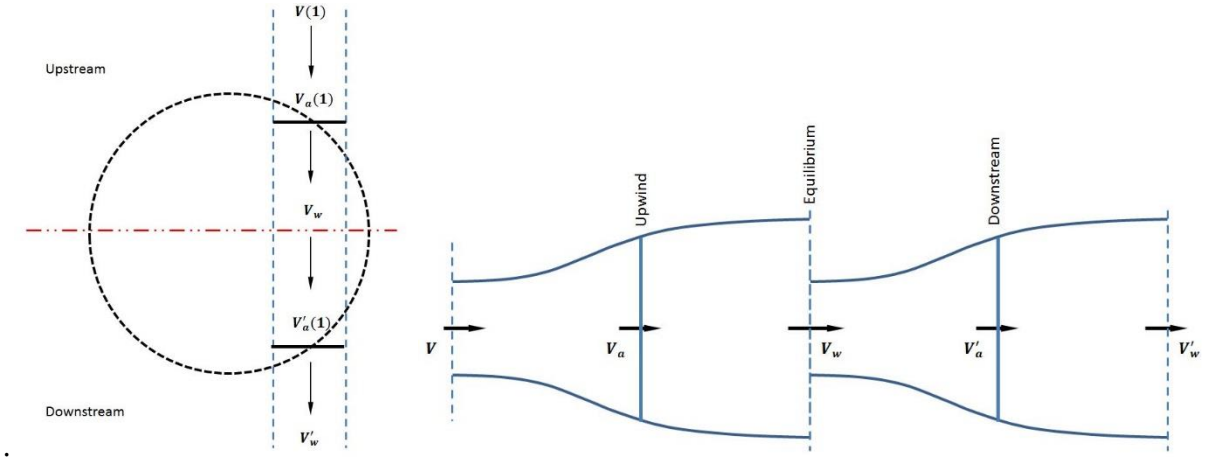

(a) (b)

Figure 13 Schematic drawing of (a) double multiple streamtube model and (b) two actuator discs in tandem [5]

In conclusion, the DMST model is currently the most widely applied analytical aerodynamic model, providing reasonably good correlation between calculated and experimental results but the model over-predicts the turbine performance under high solidity and convergence problems have been reported, especially in the downstream region and at the higher tip speed ratios [104].

3.1.2 Vortex model

Vortex models are basically potential flow models based on the calculation of the velocity field about the turbine through the influence of vorticity in the wake of the blades. Many alternative approaches to vortex modelling have been adopted but in general the turbine blades are represented by bound or lifting-line vortices (see Figure 14) whose strengths are determined using airfoil coefficient datasets and calculated using relative flow velocity and angle of attack [104].

In the context of vertical axis turbines, the 2-D vortex model was first proposed by Larsen [117] for predicting the performance of a cyclogyro windmill. Earlier studies (e.g.[117-120]) using vortex models were all based on similar principles and assumed that:

- The model only considers small angles of attack so could not be used to analyse the stall effect
- Only slightly loaded turbines are considered
- 3-D problems cannot be solved very well by using 2-D models

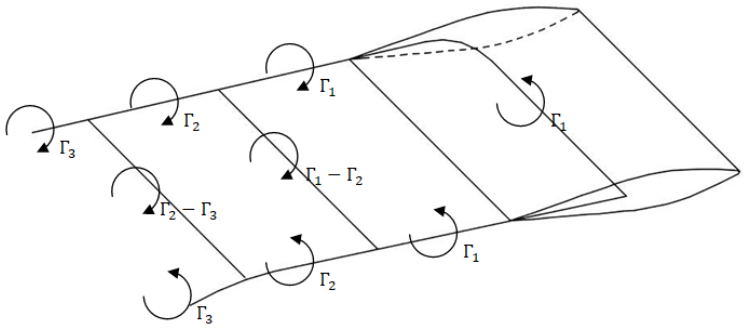

Figure 14 Vortex system for a single blade element [104]

Strickland et al.[121] presented an extension of the vortex model which included the capability of modelling 3-D effects, free wakes and dynamic stall phenomena and made further improvements[122] by incorporating the effects of dynamic stall, pitching circulation and added mass. Cardona[123] incorporated the additional effect of flow curvature as suggested by Migliore et al.[71] and found an improved correlation with the calculated and experimental results for

overall power coefficient. The main disadvantage of the vortex model is that it takes much more computation time than the BEM model [104]. Moreover, vortex models still rely on significant simplifications. For example potential flow is assumed in the wake and the effect of viscosity in the blade aerodynamics is included through empirical force coefficients [124].

Recently, Dumitrescu[125] applied the vortex model to predict and analyze the low-frequency noise produced by H-Darrieus turbines and Scheurich et al. [126] employed Brown's vortex transport model (VTM) [127] to simulate the aerodynamic performance and wake dynamics of an H-Darrieus turbine. The results from their simulation compared well with those of the experimental measurements from similar turbines.

3.1.3 Cascade model

The cascade model has been widely used to describe turbomachines and was first applied to VAWTs by Hirsch and Mandal [128]. Here, the blades of a turbine are lined up in a plane surface termed the cascade with the blade interspacing equal to the turbine's circumferential distance divided by the number of blades as shown in Figure 15. Mandal and Burton [129] improved the analytical capability of this model by taking the dynamic stall and flow curvature effects into account. According to limited studies performed in the literature, the cascade model does not suffer from the convergence problems of streamtube methods and can predict the overall values of both low and high solidity turbines reasonably well. However, the reliability of the predictions is wholly dependent on the accuracy of empirically determined parameters [104].

Recently, this model was applied by Hand and Cashman [130] and Hand et al.[131] to provide a low-cost computational design tool for studying H-Darrieus turbines to which it is well suited.

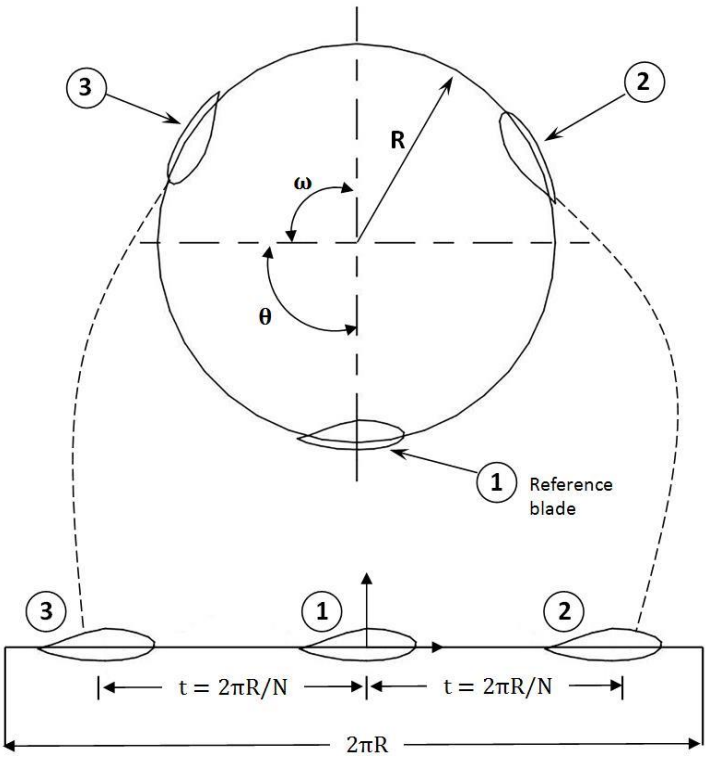

Figure 15 Cascade model configuration [104]

3.2 Computational Fluid Dynamics (CFD)

3.2.1 Turbulence model and the related studies

In the past decades, various turbulence models have been widely developed, analyzed and validated by the academic community for different applications. This section reviews the specific application of different turbulence models in studying and predicting the performance of the H-Darrieus wind turbine.

- **The $k-\varepsilon$ turbulence model**

The $k-\varepsilon$ turbulence model is numerically stable and robust therefore being applied for a wide range of turbulent flows in industrial flow and heat transfer simulations. Daroczy et al.[132] performed a detailed study of the accuracy of different turbulence models in predicting the performance of H-Darrieus turbines. By comparing the CFD results with four different experimental datasets, it was found that the Realizable $k-\varepsilon$ and $k-\omega$ SST model were the better candidates for 2D CFD. Castelli et al.[38] performed a 2D CFD study by using the Realizable $k-\varepsilon$ turbulence model and found that the maximum torque values were generated during the upwind revolution of the turbine and for azimuthal positions where rotor blades are experiencing very high relative angles of attack, even beyond the blade stall limit. It was also noted in their study that the instantaneous power coefficient locally exceeds the Betz's limit, which might result from a sudden pressure coefficient drop concerning the whole rotor disc. Howell et al.[37] employed the RNG $k-\varepsilon$ turbulence model to study the turbine performance in both two and three dimensions. Their results indicated that the 3D simulations were shown to be in reasonably good agreement with the experimental measurements while the 2D results significantly over-estimated the performance coefficient; a result that was almost entirely due to the absence of the large tip vortices that are generated in the real turbine and the 3D model. Untaroiu et al.[24] applied a standard $k-\varepsilon$ turbulence model to study the H-Darrieus turbine self-staring behaviour but both 2D and 3D models failed to accurately predict the turbine self-starting characteristic when compared to measured data. Therefore, the 3D simulation which requires significantly greater computational power and time, was not recommended by Untaroiu et al. for this particular application. Mohamed [59] examined the turbine performance with 20 different blade profiles using the Realizable $k-\varepsilon$ turbulence model and it was found that the S-1046 profile could improve the turbine maximum C_p up to 26.83% compared with NACA blades. Meanwhile Mohamed [60] also investigated the aerodynamic noise of an H-Darrieus turbine as well as the impact of blade shape, tip speed ratio, solidity and distance on noise. Their results indicated that the higher solidity and higher tip speed ratio rotors are more noisy than the normal turbines. Furthermore, Lee and Lim [133] used the RNG $k-\varepsilon$ turbulence model to numerically analyze an H-Darrieus turbine with a series of NACA blades and NACA0015 was proposed to be the optimum shape.

- **The $k-\omega$ (SST) turbulence model**

The $k-\omega$ (SST) turbulence model is a combination of superior elements of $k-\varepsilon$and $k-\omega$ turbulence models[128]. The eddy viscosity formulation is modified to take into account the effect of turbulent shear stress transportation, which is important to predict severe adverse pressure gradient flows[134]. McNaughton et al.[135] compared the 2D flow structure predicted by the $k-\omega$ SST turbulence model in its standard form and $k-\omega-$SST with a correction for low-Reynolds number effects ($k-\omega$ SST LR) and found that the low Reynolds number version correctly enabled the formation of leading edge vortices as previously observed in the literature. Edwards et al.[7] compared the blade lift coefficient predicted by four turbulence models ($S-A$, RNG $k-\varepsilon$, $k-\omega$ SST, and $k-\omega$ SST LR), which showed $k-\omega$ SST was the closest to the experimental results and that the complete cycle of the development and shedding of the dynamic stall vortex was very well predicted by the $k-\omega$ SST. Using this validated CFD model, a method of approximating the blade's local angle of attack was proposed by them. Based on the $k-\omega$ SST turbulence model, Danao et al.[136] investigated unsteady wind effects on the performance of the turbine. A fundamental relationship between instantaneous turbine performance and wind speed was revealed and it was demonstrated that the overall turbine performance could be improved under certain unsteady conditions. Bhargav et al.[137] investigated the turbine performance under fluctuating wind condition**,** demonstrating that the overall turbine performance under fluctuating wind conditions was improved when the machine was operated at higher λ with flow fluctuation frequency close to 1Hz. Amet et al.[138] studied the blade-wake interaction and demonstrated that the maximum blade lift coefficient

corresponds to the convection of vortex from leading edge to the railing edge and this vortex continues to influence the same blade at ulterior positions. Castelli et al.[139] evaluated the aerodynamic and inertial contributions to the turbine blade deformation. According to their results, the inertial contribution to the blade deformation is much higher with respect to the aerodynamic one for all the analyzed blade shell thicknesses and the displacements is higher at blade trailing edge than at leading edge. Almohammadi et al.[140] examined the blade dynamic stall of the H-Darrieus turbine using two different turbulence models and found the stall was predicted earlier when the SST transitional model was applied than for the $k-\omega$ SST and their study also revealed that the turbine performance could be improved by controlling the laminar separation bubble on the blades.

- **The SST transition turbulence model**

The SST transition turbulence model is based on the coupling of the $k-\omega$ (SST) transport equations with two other transport equations for the intermittency and the transition momentum thickness Reynolds number[134]. SST model is considered as a promising method for simulating great adverse pressure gradients and air flow separation. Arab et al.[23] studied the turbine self-starting characteristics based on the SST transition turbulence model, showing that the turbine aerodynamic performance could be affected by the history of the flow field and that the rotor inertia would affect the turbine self-starting characteristics. Balduzzi et al.[141] investigated 3D flow effects and their impacts on the energy efficiency of the turbine**.** Based on their simulation, the 3D flow effects affected blade torque by up to 8.6% and such mean torque reduction corresponds to a reduction of the effective blade length of $1.5c$. By using a 2D model, Rezaeiha et al.[142] and Rezaeiha et al.[40] examined the domain size, mesh quality and convergence for predicting the performance of H-Darrieus turbine using the SST transition turbulence model and proper guidelines were provided. Their 2.5D model, which means a certain length of blades was modelled instead of the full span, showed negligible difference with the 2D results. Meanwhile, Rezaeiha et al.[143] provided a detailed study about the impact of operational parameters (λ, Reynolds number and turbulence intensity) on the turbine performance, showing that turbine performance and wake are highly Re-dependent up to $\mathrm{Re} = 4.2 \times 10^5$ and increasing λ increased the velocity deficit, wake expansion and streamwise asymmetry in the wake. Moreover, their study also illustrated that higher turbulence intensity ($\mathrm{TI} > 5\%$) improved dynamic stall and deteriorated turbine optimal operation. Wekesa et al.[144] investigated the influence of unsteady wind for enhanced energy capture noting that the highest frequency of the wind fluctuations with meaningful energy content is of the order of 1 Hz. Lam and Peng [145] studied the wake characteristics of the turbine, which clearly revealed the asymmetrical wake in the horizontal plane using their 3D SST transition turbulence model. By comparison, their 2D model over-estimated or under-estimated the wake velocity due to the infinite blade depth and tower height. Mclaren et al.[146] investigated high solidity turbine performance also using the transition SST model demonstrating that the flow over the surface of the blade was far more complex than that observed when simply increasing or decreasing angle of attack. The generation and shedding of large vortices from the blades caused flow reversal over the blade surface and non-zero thrust loading regions, which could not be predicted by the DMST. Rossetti and Pavesi [22] adopted an improved SST model, namely SST-SAS in studying the self-starting performance of H-Darrieus VAWTs, and provided a useful comparison of the calculated results with those by using BEM theory and 2D CFD (see Table 2).

Technique	Feature
BEM model	Well documented airfoil databases at low Reynolds number is required
	Inadequate modelling of dynamics effects
	Incapable to properly simulate the turbine self-starting behaviour
2D CFD	Highlighted the presence of a complex vortices pattern
	Proved the dynamic stall effected the flow field more than the BEM model are able to
3D CFD	3D effects including secondary flow and tip effects have significantly impacts on turbine performance

Table 2 Comparison between different research approaches [22, 103]

- **Large eddy simulation (LES)**

Compared with previous models, LES requires more computing resource since larger boundary independent eddies can be directly solved through the governing equations, while smaller and more homogenous eddies are considered by using sub-grid models [103]. Li et al.[147] employed the LES model to simulate turbine performance including extreme angles of attack, which revealed that the LES model produced more realistic 3D vortex diffusion after flow separation, resulting in more accurate performance prediction. The authors also claimed that the considerably improved results achieved by the LES model implied that the poor accuracy of URANS method is mainly due to its inherent limitation in vortex modelling. Elkhoury et al.[148] assessed the effects of wind speed, turbulence intensity, blade shape and pitch angle on the turbine performance by using the LES model, and their simulation results matched well with the experimental measurements confirming the potential of LES for VAWT modelling. Patil et al.[149] performed a 3D LES simulation focused on blade dynamic stall at low tip speed ratios. The formation and detachment of six distinct leading-edge and trailing-edge vortex pairs during one rotation was clearly revealed at the expense of extremely large computer power required. Based on the LES model, Peng and Lam [150] examined the turbulence effects on the turbine wake characteristics, showing delayed dynamic stall and greater power production in the turbulent flows. Ghasemian and Nejat [151] performed an aero-acoustic prediction of the turbine using LES model, showing quadrupole noise has negligible influence on the tonal noise but the combination of thickness and loading noise are the dominant noise sources at those frequencies. Moreover, their results indicated a direct relation between the strength of the radiated noise and the rotational speed. Lei et al.[152] applied a hybrid turbulence model, the Improved Delayed Detached Eddy Simulation (IDDES) to study the performance of two-bladed H-Darrieus turbine, which showed good agreement with the experimental measurements. According to Lei et al.'s[152] results, it was found the vortices around the blades predicted by the IDDES model were richer and more realistic than those obtained by the $k-\omega$ SST model, especially when the blades undergo dynamic stall.

All in all, there is no simple conclusion as to which turbulence model is best for this specific application, nor whether there is an optimal compromise between computational power requirement and accuracy. At the time of writing the LES model seems to provide the best agreement with experimental results but at the expense of huge computing power and run time. A summary of useful CFD studies is provided in the Table 3.

Turbulence model	Author	Method	Reynolds number ($\times 10^4$)*	Focus/Topic
$k-\varepsilon$	Daroczy et al. [132]	2D	2.0~27.0	Comparison of different turbulence model
	Castelli et al. [38]	2D	5.2	Correlation between flow characteristics to rotor torque and power
	Howell et al. [37]	2D and 3D	2.1~3.7	Numerical prediction of turbine performance and the associated flow characteristics
	Untaroiu et al. [24]	2D and 3D	3.4	Turbine self-starting behaviour
	Mohamed[59]	2D	N/A	Turbine performance with different blade
	Mohamed[60]	2D	N/A	Aerodynamic noise of the turbine
	Lee and Lim[133]	3D	8.1~16.2	The optimum shape of the Darrieus-type wind turbine
$k-\omega$	McNaughton et al. [135]	2D	15.0	Comparison of different turbulence model on the prediction of turbine flow structure
	Edwards et al. [7]	2D	1.8	Comparison of different turbulence model and investigation of turbine aerodynamics
	Danao et al. [136]	2D	N/A	Influence of unsteady wind on the performance and aerodynamics of a vertical
	Meana-Fernandez et al. [98]	2D	6.8~10.1	Effect of design parameters on the turbine performance
	Bhargav et al. [137]	3D	~30.4	The turbine performance under fluctuating wind condition
	Amet et al. [138]	2D	0.3	Blade-Vortex Interaction
	Castelli et al. [139]	3D	5.2	Aerodynamic and inertial contributions to a vertical-axis wind turbine blade deformation.
	Almohammadi et al. [140]	2D	28.3	Dynamic stall
SST Transition	Arab et al. [23]	2D	4.7~16.9	Turbine self-starting behaviour and aerodynamic performance
	Balduzzi et al. [141]	3D	5.2	Blade unsteady aerodynamics
	Rezaeiha et al. [142, 153]	2D and 2.5D	3.8	Domain size, mesh quality and convergence for predicting the turbine performance
	Rezaeiha et al. [143]	2D and 2.5D	3.8	Impact of operational parameters on the turbine performance.
	Wekesa et al. [144]	2D	3.0	Unsteady wind for enhanced energy capture.
	Lam and Peng[145]	2D and 3D	3.8	Wake characteristics
	Mclaren et al. [146]	2D	36.4	Complex flow–blade interaction mechanisms
	Rossetti and Pavesi[22]	2D and 3D	3.4	Turbine start-up characteristics
LES	Li et al. [147]	2.5D	30.0	High angle of attack flow
	Elkhoury et al. [148]	3D	8.1	Wind speed, turbulence intensity, blade shape
	Patil et al. [149]	3D	4.1	Flow filed and aerodynamics of the turbine
	Peng and Lam[150]	3D	3.1	Turbulence effects on the wake characteristics and turbine aerodynamic performance
	Ghasemian and Nejat[151]	3D	5.5	Aerodynamic noise radiated from turbines
	Lei et al. [152]	3D	50.7	Turbine aerodynamics including the wake

*The Reynolds number is calculated based on the upstream wind speed.

Table 3 Summary of typical CFD studies in terms of different turbulent models

3.3 Experimental measurements

Although experimental research and development can be conducted in wind tunnels or in the field, almost all of the VAWT research that provides detailed flowfield data has been focused on model wind tunnel testing. Initially measurements were based on global parameters such as power and speed under either at steady state (or time averaged) conditions or slow transients. These have since been supplemented by point measurements (time averaged and instantaneous) using research tools such as fast response pressure probes or thermal anemometry and more recently data from techniques including PIV and on-board scanning have further contributed to our understanding

Unlike large HAWTs which are deliberately located in exposed locations where there is a clearly defined ground boundary layer, small-scale VAWTs are much more likely to be located in or around urban or industrial sites, each with unique wind characteristics. Only recently have researchers started to consider replicating the individual onset flow conditions in terms of both time-averaged wind velocity profile and time resolved unsteady wind structures. A comprehensive review of existing and new developments for generating these effects in the wind tunnel has been provided by Mankowski[154].

3.3.1 Traditional wind tunnel measurement

The first wind tunnel research programmes for VAWT applications were used to obtain the turbine's characteristic operating curves as the basis for machine design under various steady wind conditions. For example, Mazarbhuiya et al.[155] investigated a turbine's performance using different asymmetric blades with a focus on the influence of blade aspect ratio whilst specialist facilities enable the breadth of experimentation to be expanded as exemplified by Weber et al.[156] who studied turbine noise in the wind tunnel with a 1/2-inch free-field microphones. They showed that the main sources of the H-Darrieus sound pressure field were the separation-stall and the blade vortex interaction. Molina et al.[157] examined the time-resolved turbine near wake velocity under turbulent flow by using a traversing hot-wire probe. An improved turbine performance under turbulent flow was found to relate to faster wake recovery and the reduced shaft wake. Bianchini et al.[158] studied both the global turbine performance and the wake structure using a combination of a torque meter, wind speed and hot wire anemometer. The velocity values measured experimentally in the wake compared well with their CFD predictions and the experiment provides a useful source of CFD validation data. Eboibi et al.[47] applied an optical encoder to record turbine's rotational speed and acceleration which used together with the turbine's known moment of inertia allowed torque and power to be derived. Armstrong et al.[99] investigated the flow separation on a high Reynolds number, high solidity H-Darrieus turbine by recording the motion of light-weight tufts which were attached to the inner surface of a blade. Conventional wind tunnel measurement techniques have also been used to evaluate innovative flow control techniques. For example, Greennblatt et al.[159] examined the turbine performance with dielectric barrier discharge plasma actuators installed on the blade leading edges and demonstrated a 38% power improvement. Peng et al.[160] studied the wake aerodynamics of a five-bladed H-Darrieus turbine using a four-hole cobra probe and a laser displacement sensor for recoding the rotational speed. Published information from many wind tunnel studies using traditional techniques to study the turbine performance is widely available (e.g. references [5, 30, 37, 95, 102, 148, 161-165]) and a summary table is provided in Table 4.

Author	Method	Blade profile	Solidity	Reynolds number ($\times 10^4$)*	Focus/Topic
Mazarbhuiya et al.[155]	Tachometer, dynamometer	NACA-63415	0.60	1.3~2.0	The turbine performance with asymmetric blades
Weber et al.[156]	Microphones, hysteresis brake	NACA0018	1.50	2.8	Noise measurement and numerical model validation
Molina et al.[157]	Torque sensor, DC motor, Pitot tube, hot-wire probe	NACA0018	N/A	3.0	Turbine near wake under turbulent flow
Bianchini et al. [158]	Torque meter, hot wire, five-hole probe	NACA0021	0.50	N/A	Turbine performance and wake structure
Eboibi et al. [47]	Optical encoder, hot-wire anemometer	NACA0022	0.26, 0.34	1.2~2.1	Effect of solidity on the turbine performance
Armstrong et al. [99]	Tufts, video camera	NACA0015	0.88	30	Flow separation behaviour on the straight blades
Greennblatt et al. [159]	Dynamometer, plasma actuators	NACA0015	1.25	4.4~7.1	Turbine performance with plasma actuators installed on the blade leading edges
Peng et al. [160]	Four-hole cobra probe, hot-wire probe,	N/A	1.50	3.4	Turbine near and mid-range wake measurement
Singh et al. [30]	Dynamometer, anemometer	S1210	1.60, 2.40	2.6~5.9	Turbine self-starting and overall performance
Howell et al. [37]	Tachometer, torque brake	NACA0022	0.67, 1.00	2.1~3.7	The effect of solidity and blade surface roughness on the turbine performance
Li et al. [94]	Clay, digital torque detector	NACA0018	0.70	2.4~3.1	The effect of attachment on the turbine performance
Danao et al. [101]	Hot wire, hysteresis brake, DC motor, optical encoder	NACA0022	0.34	1.6~2.2	The influence of unsteady wind on the turbine performance
Elkhoury et al. [147]	Induction motor, torque transducer, tachometer, pitot tube, anemometer	NACA634-221 NACA0018 NACA0021	1.50	0.8~1.1	The effect of wind speed, turbulence intensity, blade profile, pitch angle on the turbine performance
Elkhoury et al. [161]	Ultrasonic anemometer, hot-wire probe ,	N/A	0.67, 0.85, 1.20,	16~28	Performance of a Orthopter-type VAWT
Battist et al. [162]	Torquemeter, hot-wire probe	NACA0021	0.50	5.1	Mid-span wake and overall performance
Du et al.[165]	Optical sensor, motor	NACA0021 NACA4415 DU06W200	1.0, 0.81, 0.67	4.7	Effects of various design parameters on turbine self-starting and overall performance

*The Reynolds number is calculated based on the upstream wind speed.

Table 4 Summary of typical traditional wind tunnel tests

3.3.2 2D and 3D Optical Measurements

The availability of single and multiple planes, quantitative data obtained primarily from Particle Image Velocimetry (PIV), has provided valuable supplementary information that helps the researcher to visualise flowfield development using images that can be matched to their CFD counterparts. The PIV approach as shown in Figure 16 enables researchers to observe the instantaneous 2D planar flow in detail at any position in the flowfield where there is optical access. Measurement in the third dimension is also possible although measurement accuracy in the third dimension is generally less reliable. The technique therefore allows across the rotor and wake for the time-averaged or time-resolved measurement of velocity field that would be difficult and often impossible using conventional probes. Although high speed PIV systems are now available commercially, the frequencies that can be achieved are insufficient to capture in real time the full wake characteristics of a VAWT model at its design tip speed ratio. A more realistic approach is the use of the phase averaging techniques to explore 'instantaneous' events as adopted by most previous studies.

Fujisawa et al.[166] observed the dynamic stall of an H-Darrieus turbine by using the particle image velocimetry (PIV) measurement as shown in Figure 17. Based on their observation, it was found that the mechanism of dynamic stall was due to the successive generation of flow separation on the inner surface of the blade followed by the formation of roll-up vortices from the outer surface. Posa et al.[167] studied the wake structure of the turbine and found that the tip speed ratio was an important parameter in determining the characteristic of VAWTs wakes at high Reynolds number. An example of valuable data that has been derived from 2D PIV is that of Ferreira et al.[168] who were able to focus on dynamic stall structures and the evolution of the flow around the blade while the extension to 3D structures is typified by the work of Tescione et al.[169] who analyzed the wake flow by using the stereoscopic particle image Velocimetry (SPIV), revealing the evolution of the blade's tip vortices and the asymmetry of the wake, both in its horizontal expansion and vertical development. Rolin and Porte-Agel [170] also studied the turbine wake using SPIV and the presence of two pairs of counter-rotating vortices at the edges of the wake was observed. Buchner et al.[171] compared their SST simulation results of blade dynamic stall with the SPIV measurement, which showed good agreement. The application of PIV for VAWT research is not confined to wind tunnels and Rolland et al.[172] performed a PIV study about a small VAWT in a marine current flume tank and their CFD model using $k-\omega$ (SST) turbulence model successfully captured the physics of the flow. Hohman et al.[173] employed the SPIV to investigate the effect of inflow conditions on the turbine wake behaviour, finding that the inflow turbulence did not significantly affect the overall wake structure. Their study also demonstrated that the wake decays rapidly downstream with significant momentum recovery and turbulence reduction after three turbine diameters. A summary table of some valuable PIV tests is provided in Table 5. Some similar studies by using Acoustic Doppler Velocimeter (ADV), Laser Doppler Velocimetry (LDV) and magnetic resonance velocimetry (MRV) for studying the H-Darrieus turbine flow could be also found in reference [174] , references[164, 175, 176] and reference [177] respectively.

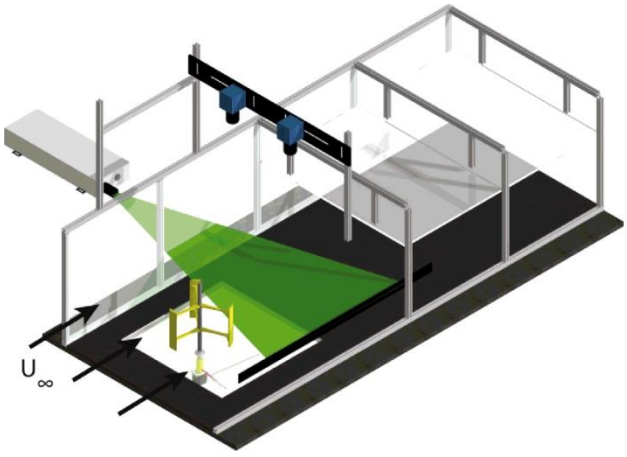

Figure 16 Schematic of typical PIV set-up [167]

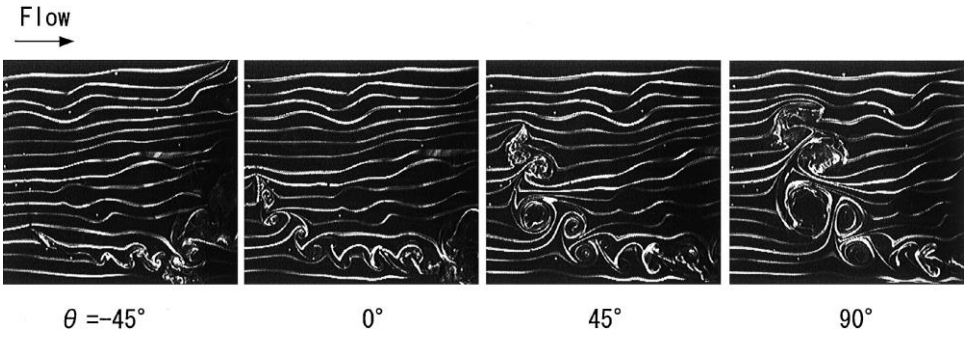

Figure 17 Flow visualization of dynamic stall of H-Darrieus wind turbine [166]

Author	Method	Blade profile	Solidity	Reynolds number ($\times 10^4$)*	Focus/Topic
Fujisawa and Shibuya[166]	PIV, flow visualization	NACA0018	0.33	0.3	Dynamic stall on the turbine blade
Posa et al. [167]	PIV	NACA0022	1.00	3.0	Wake structure of an isolated VAWT
Ferreira et al. [168]	PIV	NACA0015	0.25	1.8~3.5	Dynamic stall and shedding of vorticity
Tescione et al. [169]	SPIV	NACA0018	0.24	3.8	Near wake characteristics
Rolin and Porte-Agel[170]	SPIV	NACA0018	1.08	1.9	Wake structure in boundary layer flow
Buchner et al. [171]	SPIV	N/A	0.60	2.3~6.9	Dynamic stall and validation of CFD model
Rolland et al. [172]	PIV	N/A	N/A	N/A	Performance assessment and model validation
Hohman et al. [173]	SPIV	NACA0020	0.30	2.4~12.7	The effects of inflow conditions on vertical axis wind turbine wake structure and performance

*The Reynolds number is calculated based on the upstream wind speed and blade chord length

Table 5 Summary of typical PIV tests

3.3.3 On-board pressure measurement

It is difficult to measure the pressure variation around the surface of H-Darrieus wind turbine blades using traditional methods such as hot wires or pressure probes due to the rotating nature of the turbine. Traditionally, slip rings have been adopted for the transmission of power and signals to and from rotating machinery but for model wind tunnel studies of VAWTs they can introduce unwanted inertial effects which influence starting performance, flow blockage leading to incorrect onset wind direction and turbine through flow, and electronic noise which can mask small changes in signal output. With the advent of accessible microelectronics, miniature on-board measurement and data storage devices has been developed (e.g. Du et al.[5, 79] and Li et al.[178]) where all of the measuring and recording components were placed on the turbine and rotated along with the blades. In order to obtain time-accurate pressure data the frequency response of the pressure sensors must be adequate and if tubing is used to connect the sensors to pressure

tappings or a probe head then the transfer function must have a form that can allow for the reliable correction of signal phase and attenuation. The former is not usually a concern with modern, miniature transducers. For example, the pressure scanner used by Du et al.[79] can be used at frequencies up to 20,000Hz. Transfer function corrections for tube lengths of up to 0.5m can typically be applied for frequencies up to around 500Hz (e.g. SimsWilliams[179, 180]) which is just sufficient for most model wind tunnel VAWT experiments.

In Du et al.'s study [5, 79], an instrumented NACA0021 blade was assembled from a set of laser cut plywood laminates of 10 mm width. In addition to the wooden laminates a single perspex laminate was constructed which housed 15 surface static pressure tappings as shown in Figure 18. A microcontroller datalogger was developed to record the instantaneous pressure variation around the blade via a 16-channel miniature electronic pressure scanner. All the components were attached to the turbine and controlled wirelessly using Bluetooth technology as shown in Figure 19. The time interval between each measurement was pre-set to record 1,440 points for one revolution (a constant angular step of $\theta = 0.25^{\circ}$) and the sampling frequency ranges from $\sim$2600Hz to $\sim$10000Hz for different turbine tip speed ratios. Although the on-board pressure measurement system is able to obtain the time-resolved pressure data, the time-averaged results were presented in order to minimize any experimental error or system error. By using this approach, flow characteristics including dynamic stall, laminar separation bubbles and vortex convection along the blade were clearly observed [79].

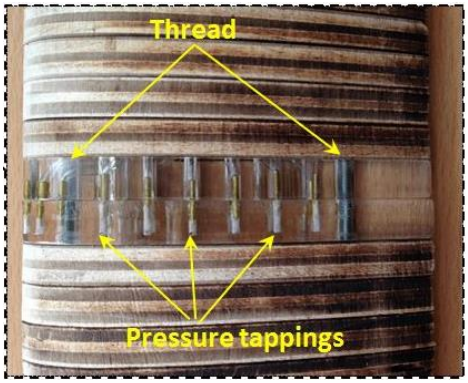

Figure 18 The NACA0021 blade with the pressure tapping section made from perspex [5]

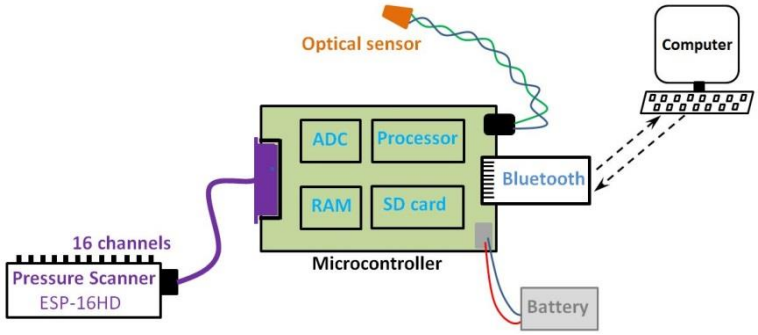

Figure 19 Schematic diagram of the microcontroller datalogger and other components [5]

In the study of Li et al.[178], a set of NACA0015 blades was equipped with a total of 32 pressure taps with measurements repeated at several spanwise locations. The devices were controlled wirelessly by a remote computer as shown in Figure 20. The pressure measurements were averaged over a number of rotations using a bin averaging technique with a bin size of 5 degree. Their numerical simulations of the blade pressure distribution matched well with the experiment measurements and their study also illustrated that the turbine power coefficient could be significantly improved by reducing the 3-D effects of the blade and its support structures.

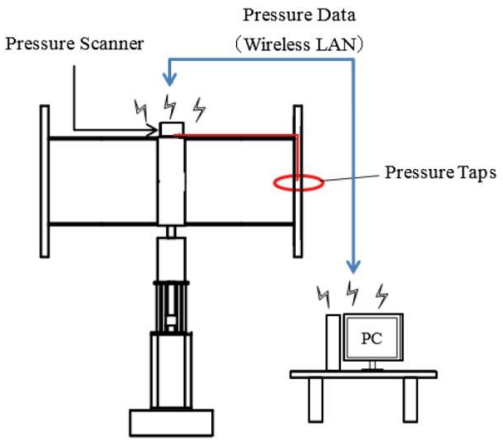

Figure 20 Schematic diagram of the pressure measurement principle [178]

Author	Method	Blade profile	Solidity	Reynolds number ($\times 10^4$)*	Focus/Topic
Du et al.[79]	On-board pressure measurement	NACA0021	1.00	4.7	Dynamic pressure variation around the turbine blade
Li et al. [178]	On-board pressure measurement	NACA 0015	0.53	10.6	Blade pressure distribution at different spanwise locations
*The Reynolds number is calculated based on the upstream wind speed and blade chord length					

Table 6 Summary of the two on-board pressure measurement tests

4. Conclusions

This review provides an overview of the development, knowledge and understanding of H-Darrieus wind turbine aerodynamics including design considerations, research approaches and research tools. Particular focus is put on the crucial challenge of design a turbine that could self-start. Conclusions can be drawn as follow:

- Important parameters have been identified which significantly influence a turbine's performance including its ability to self-start and to quickly accelerate to near-optimal steady state performance. Those parameters, which should be considered during the design stage include, but are not limited to, turbine solidity, blade number, blade profile, flow curvature effects, pitch angle, surface roughness and Reynolds number. It has been observed that for many design aspects there is a need for further research and discussion before clear conclusions can be agreed.
- The main approaches to analytical modelling are introduced and their relative strengths and weaknesses are discussed. These include Momentum, Vortex and Cascade-based models that provide low-cost computational design tools but despite continual development they remain limited by the assumptions and simplifications that are required. Moreover, a well-documented aerofoil database at appropriate Reynolds range is the prerequisite for studies using analytical models
- Currently, CFD is the most widely used method for studying these turbines. Different turbulence models including $k-\varepsilon$, $k-\omega$ (SST), SST transition and LES have been adopted by different researchers but currently there remains no clear conclusion as to which turbulence model is the best and a compromise between accuracy and computing resource is often required. It is generally accepted that the LES model provides the best agreement with experimental results but at the expense of a high demand for computer

power and time that is often out of the reach of industrial design teams. Except for some fundamental research topics, 2D CFD has limited value and 3D modelling has become an essential tool.

- Experimental measurements continue to provide the data against which analytical and numerical methods are validated although high quality, time accurate data remain scarce. Traditional wind tunnel measure still presents a popular method to obtain turbine's characteristic operating curves as the basis for machine design under various steady wind conditions. Measurements are based on global parameters such as power and speed under either steady state (or time averaged) conditions or slow transients. In recently years, advanced techniques such as PIV and on-board pressure measurements are becoming more widely used to visualise flowfield development and to obtain the instantaneous pressure distribution around the blade during turbine operation. It is anticipated that with those advances will come greater understanding of the flow physics associated with H-Darrieus wind turbines and of their potential to contribute to the world's renewable energy supply.

5. Future study

Some possible future research directions from the turbine aerodynamic perspective are provided here:

- Blades with modified leading edges present promising candidates for future application. Studies should be performed to test the turbine performance with these blades and further improve the blade configuration based on the understanding of the flow physics.
- With the development of computer technology, 3D LES models should be further applied to explore the turbine transient self-starting process and examine the 3D effects that are responsible for the differences that are currently observed between experimental measurements and 2D simulations.
- The aerodynamic interaction among turbines placed in arrays or rows should be further examined using 3D CFD and PIV techniques. Optimum parameters including wake recovery distance would be valuable for future applications.
- For small-scale application at low Reynolds number ($\mathrm{Re} = \sim 10^5$), the unique aerodynamic behaviour of individual blades including vortex convection could be further investigated.
- High frequency, real-time data should be obtained to further our understanding of the flow physics of rotating machines.
- Consideration should be given to testing VAWT models in representative conditions of wind shear and atmospheric turbulence.

References

1. Bos R. *Self-starting of a small urban Darrieus rotor*. Master of Science Thesis, Delft University of Technology, Netherland, 2012.
2. Sutherland H, Berg DE and Ashwill TD. A Retrospective of VAWT Technology. *SAND2012-0304, United States* 2012.
3. Wilson RE, and Lissaman PBS. Applied Aerodynamics of Wind Power Machine, NTIS Report Pb-238595, 1974.
4. Gouriérès DL. *Wind Power Plants Theory and Design*. Headington Hill Hall: Pergamon Press Ltd, 1982.
5. Du L. *Numerical and Experimental Investigations of Darrieus Wind Turbine Start-up and Operation*. PhD Thesis, Unverisity of Durham, UK, 2016.
6. Bertenyi T, Wickins C and Mcintosh SC. Enhanced Energy Capture Through Gust-Tracking in the Urban Wind Environment. *48th AIAA Aerospace Sciences Meeting Including the New Horizons Forum and Aerospace Exposition*. Orlando, Florida, USA, 4 - 7 January 2010, Paper No. AIAA 2010–1376.
7. Edwards JM, Danao LA and Howell RJ. Novel Experimental Power Curve Determination and Computational Methods for the Performance Analysis of Vertical Axis Wind Turbines. *J Sol Energy Eng* 2012; 134.
8. Mertens S, Van Kuik G and Van Bussel G. Performance of an HDarrieus in the Skewed Flow on a Roof. *J Sol Energy Eng* 2003; 125: 433-440.
9. Dabiri JO. Potential order-of-magnitude enhancement of wind farm power density via counter-rotating vertical-axis wind turbine arrays. *Renewable and Sustainable Energy Reviews* 2011; 3.
10. Kinzel M, Mulligan Q and Dabiri JO. Energy exchange in an array of vertical-axis wind turbines. *Turbulence* 2012; 13: 1-13.
11. Tjiu W, Marnoto T, Mat S, et al. Darrieus vertical axis wind turbine for power generation I: Assessment of Darrieus VAWT configurations. *Renewable energy* 2015; 75: 50-67.
12. Tummala A, Velamati RK, Sinha DK, et al. A reviewonsmallscalewindturbinesc. *A reviewonsmallscalewindturbines* 2016; 56: 1351-1371.
13. Kirke BK. *Evaluation of Self-Starting Vertical Axis Wind Turbines for Stand-Alone Applications*. PhD Thesis, School of Engineering, Griffith University, Australia, 1998.
14. Ebert PR, and Wood DH. Observations of the starting behaviour of a small horizontal-axis wind turbine. *Renewable Energy* 1997; 12: 245-257.
15. Lunt PAV. *An aerodynamic model for a vertical-axis wind turbine*. MEng Project Report, School of Engineering, University of Durham, UK, 2005.
16. Worasinchai S, Ingram GL and Dominy RG. The Physics of H-Darrieus Turbine Starting Behavior. *J Eng Gas Turbine Power* 2016; 138.
17. Hill N, Dominy RG, Ingram G, et al. Darrieus Turbines: the Physics of Self-starting. *Proceedings of the Institution of Mechanical Engineers, Part A: Journal of Power and Energy* 2008; 223: 21-29.
18. Dominy RG, Lunt P, Bickerdyke A, et al. Self-Starting Capability of a Darrieus Turbine. *Proceedings of the Institution of Mechanical Engineers, Part A: Journal of Power and Energy* 2012; 221: 111-120.
19. Baker JR. Features to Aid or Enable Self Starting of Fixed Pitch Low Solidity Vertical Axis Wind Turbines. *Wind Engineering and Industrial Aerodynamics* 1983; 15: 369-380.
20. Du L, Berson A and Dominy RG. The prediction of the performance and starting capability of H-Darrieus wind turbines. *ASME Turbo Expo*. Montreal, Canada, 15-19 June 2015, Paper No. GT2015-4221.
21. Somoano M, and Huera-Huarte FJ. The dead band in the performance of cross-flow turbines: Effects of Reynolds number and blade pitch. *Energy Convers Manag* 2018; 172: 277-284.
22. Rossetti A, and Pavesi G. Comparison of Different Numerical Approaches to the Study of the H-Darrieus Turbines Start-Up. *Renewable Energy* 2013; 50: 7-19.
23. Arab A, Javadi M, Anbarsooz M, et al. A numerical study on the aerodynamic performance and the selfstarting characteristics of a Darrieus wind turbine considering its moment of inertia. *Renewable Energy* 2017; 107: 298-311.
24. Untaroiu A, Wood H, Allaire PE, et al. Investigation of Self-Starting Capability of Vertical Axis Wind Turbines Using a Computational Fluid Dynamics Approach [J]. *J Sol Energy Eng* 2011; 133.
25. Batista NC, Melicio R, Mendes VMF, et al. On a self-start Darrieus wind turbine:Blade design and field tests. *Renewable and Sustainable Energy Reviews* 2015; 52: 508-522.
26. Dumitrescu H, Dumitrache A, Popescu CL, et al. Wind Tunnel Experiments on Vertical-Axis Wind Turbines with Straight Blades. *International Conference on Renewable Energies and Power Quality*. Cordoba, Spain, 8-10 April 2014.
27. Asr MT, Nezhad EZ, Mustapha F, et al. Study on start-up characteristics of H-Darrieus vertical axis wind turbines comprising NACA 4-digit series blade airfoils. *Energy* 2016; 112: 528-537.

28. Douak M, Aouachria Z, Rabehi R, et al. Wind energy systems: Analysis of the self-starting physics of vertical axis wind turbine. *Renewable and Sustainable Energy Reviews* 2018; 81: 1602-1610.
29. Sengupta AR, Biswas A and Gupta R. Studies of some high solidity symmetrical and unsymmetrical blade H-Darrieus rotors with respect to starting characteristics, dynamic performances and flow physics in low wind streams. *Renewable Energy* 2016; 93: 536-547.
30. Singh MA, Biswas A and Misra RD. Investigation of self-starting and high rotor solidity on the performance of a three S1210 blade H-type Darrieus rotor. *Renewable Energy* 2015; 76: 381-387.
31. Templin RJ. *Aerodynamic Performance Theory for the NRC Vertical-Axis Wind Turbine*. National Research Council of Canada. Laboratory technical report ; LTR-LA-160, 1974.
32. Blackwell BF, Sheldahl RE and Feltz LV. *Wind Tunnel Performance Data for the Darrieus Wind Turbine with NACA0012 Blades*. Sandia Laboratories, SAND76-0130, 1977.
33. Consul CA, Willden RHJ, Ferrer E, et al. Influence of Solidity on the Performance of a Cross-Flow Turbine. *Proceedings of the 8th European Wave and Tidal Energy Conference* Uppsala, Sweden, January2009.
34. Gosselin R, Dumas G and Boudreau M. Parametric study of H-Darrieus vertical-axis turbines using CFD simulations. *Renewable and Sustainable Energy* 2016; 8.
35. Vassberg JC, Gopinath AK and Jameson A. Revisiting the Vertical-Axis Wind Turbine Design Using Advanced Computational Fluid Dynamics. *43rd AIAA Aerospace Sciences Meeting and Exhibit*. Reno, Nevada, USA, 10-13 January 2005.
36. Worstell MH. *Aerodynamic Performance of the 17-m-Diameter Darrieus Wind Turbine in the Three-Bladed ConVguration: An Addendum*. Sandia Laboratories, SAND-79-1753, 1982.
37. Howell R, Qin N, Edwards J, et al. Wind Tunnel and Numerical Study of a Small Vertical Axis Wind Turbine. *Renewable Energy* 2010; 35: 412-422.
38. Castelli MR, Englaro A and Benini E. The Darrieus Wind Turbine: Proposal for a New Performance Prediction Model Based on CFD. *Energy* 2011; 36: 4919-4934.
39. Subramanian A, Yogesh SA, Sivanandan H, et al. Effect of airfoil and solidity on performance of small scale vertical axis wind turbine using three dimensional CFD model. *Energy* 2017; 133: 179-190.
40. Rezaeiha A, Montazeri H and Blocken B. Towards optimal aerodynamic design of vertical axis wind turbines: Impact of solidity and number of blades. *Energy* 2018; 165: 1129-1148.
41. Li Q, Maeda T, Kamada Y, et al. Effect of solidity on aerodynamic forces around straight-bladed vertical axis wind turbine by wind tunnel experiments (depending on number of blades). *Renewable Energy* 2016; 96: 928-939.
42. Sagharichi A, Zamani M and Ghasemi A. Effect of solidity on the performance of variable-pitch vertical axis wind turbine. *Energy* 2018; 161: 753-775.
43. Kirke BK, and Lazauskas L. Enhancing the Performance of a Vertical Axis Wind Turbine Using a Simple Variable Pitch System. *Wind Engineering* 1991; 15: 187-195.
44. Musgrove PJ, and Mays ID. Development of the Variable Geometry Vertical Axis Windmill. *International Symposium on Wind Energy Systems*. Amsterdam, Netherlands, 3-6 October 1978
45. Roh SC, and Kang SH. Effects of a blade profile, the Reynolds number, and the solidity on the performance of a straight bladed vertical axis wind turbine. *Journal of Mechanical Science and Technology* 2013; 27: 3299-3307.
46. Simhan K. *A Review of Calculation Methods for the Determination of Performance Characteristics of Vertical Axis Wind Energy onverters with Special Reference to the Influence of Solidity and Starting Characteristics*. Bremen Univiversity. Fachberichte Physik. Report No. 12, 1984.
47. Eboibi O, Danao LAM and Howell RJ. Experimental investigation of the influence of solidity on the performance and flow field aerodynamics of vertical axis wind turbines at low Reynolds numbers. *Renewable Energy* 2016; 92: 474-483.
48. Corporation F. *Final Project Report: High-Energy Rotor Development Test and Evaluation*. Sandia Laboratories, SAND96-2205, 1996.
49. Mcintosh SC. *Wind Energy for the Built Environment*. PhD thesis, Cambridge University, UK, 2009.
50. Sabaeifard P, Razzaghi H and Forouzandeh A. Determination of Vertical Axis Wind Turbines Optimal Configuration through CFD Simulations *2012 International Conference on Future Environment and Energy*. Singapoore, 2012.
51. Berg DE. *Customised Airfoils and Their Impact on VAWT Cost of Energy*. Sandia Laboratories, SAND90-1148C, 1990.
52. Klimas PC. *Tailored Airfoils for Vertical Axis Wind Turbines. Sandia Laboratories*. Sandia Laboratories, SAND84-1062, 1992.
53. Masson C, Leclerc C and Paraschivoiu I. Appropriate Dynamic-Stall Models for Performance Predictions of VAWTs with NLF Blades [J]. *International Journal of Rotating Machinery* 1998; 4: 129-139.

54. Angell RK, Musgrove PJ and Galbraith RAMcD. Unsteady wind tunnel testing of thick section aerofoils for use on large scale veritcal axis wind turbine. *Wind energy Conversion, Proceeding of 10th BWEA conferecne*. London, UK, 22-24 March 1988, p. 195-203.
55. Islam M, Ting DSK and Fartaj A. Desirable Airfoil Features for Smaller Capacity Straight Bladed VAWT. *Wind Engineering* 2007; 31: 165-196.
56. Bianchini A, Ferrari L and Magnani S. START-UP BEHAVIOR OF A THREE-BLADED H-DARRIEUS VAWT: EXPERIMENTAL AND NUMERICAL ANALYSIS. *Asme Turbo Expo* 2011; 6: 811-820.
57. Bausas MD, and Danao LAM. The aerodynamics of a camber-bladed vertical axis wind turbine in unsteady wind. *Energy* 2015; 93: 1155-1164.
58. Chen C-C, and Kuo C-H. Effects of pitch angle and blade camber on flow characteristics and performance of small-size Darrieus VAWT. *J Vis (Tokyo)* 2013; 16: 65-74.
59. Mohamed MH. Performance Investigation of H-Rotor Darrieus Turbine With New Airfoil Shapes. *Energy* 2012; 47: 522-530.
60. Mohamed MH. Aero-acoustics noise evaluation of H-rotor Darrieus wind turbines. *Energy* 2014; 65: 596-604.
61. Claessens M. The Design and Testing of Airfoils for Application in Small Vertical Axis Wind Turbines. *Master thesis, Faculty of Aerospace Engineering, Delft University of Technology, Netherlands* 2006.
62. Ikonwa CA, Gale WF and Ingham DB. Investigation of airfoil profiles for use in self-starting, small-scale, low reynolds number vertical axis wind turbines. *The International Journal of Environmental Sustainability* 2016; 12: 33-52.
63. Woodward BL, Winn JP and Fish FE. Morphological Specializations of Baleen Whales Associated With Hydrodynamic Performance and Ecological Niche. *J Morphol* 2006; 267: 1284-1294.
64. Miklosovic DS, Murray MM, Howle LE, et al. Leading Edge Tubercles Delay Stall on Humpback Whale Flippers. *Phys Fluids* 2004; 16: 39-42.
65. Van Nierop EA, Alben S and Brenner MP. How Bumps on Whale Flippers Delay Stall: an Aerodynamic Model. *Phys Rev Lett* 2008; 100: 054502.
66. Hansen KL, Kelso RM and Dally BB. Performance Variations of Leading-Edge Tubercles for Distinct Airfoil Profiles. *AIAA J* 2011; 49: 185-194.
67. Wang Z, and Zhuang M. Leading-edge serrations for performance improvement on a vertical-axis wind turbine at low tip-speed-ratios. *Appl Energy* 2017; 208: 1184-1197.
68. Wang Z, Wang Y and Zhuang M. Improvement of the aerodynamic performance of vertical axis wind turbines with leading-edge serrations and helical blades using CFD and Taguchi method. *Energy Convers Manag* 2018; 177: 107-121.
69. Hashem I, and Mohamed MH. Aerodynamic performance enhancements of H-rotor Darrieus wind turbine. *Energy* 2018; 142: 531-545.
70. Ma N, Lei H, Han Z, et al. Airfoil optimization to improve power performance of a high-solidity vertical axis wind turbine at a moderate tip speed ratio. *Energy* 2018; 150: 236-252.
71. Migliore PG, Wolfe WP and Fanucci JB. Flow Curvature Effects on Darrieus Turbine Blade Aerodynamics. *Energy* 1980; 4: 49-55.
72. Rainbird JM, Bianchini A, Balduzzi F, et al. On the influence of virtual camber effect on airfoil polars for use in simulations of Darrieus wind turbines. *Energy Convers Manag* 2015; 106: 373-384.
73. Sharpe DJ. Refinements and developments of the multiple streamtube theory for the aerodynamic performance of vertical axis wind turbines. *In Proceedings of the BWEA Wind Energy Conference*. 1984.
74. Paraschivoiu I, and Delclaux F. Double-Multiple Streamtube Model With Recent Improvements. *AIAA J* 1983; 7: 250-255.
75. Paraschivoiu I, Frauni P and Beguier C. Streamtube Expansion Effects on The Darrieus Wind Turbine. *AIAA J* 1985; 1: 150-155.
76. Paraschivoiu I. Double-Multiple Streamtube Model for studying Vertical Axis Wind Turbine. *AIAA J* 1987; 4: 370-377.
77. Soraghan CE, Leithead WE, Feuchtwang J, et al. Double Multiple Streamtube Model for Variable Pitch Vertical Axis Wind Turbines [J]. *31st AIAA Applied Aerodynamics Conference*. San Diego, USA, 24-27 June 2013.
78. Goude A. *Fluid Mechanics of Vertical Axis Turbines*. PhD thesis, Uppsala University, Sweden, 2012.
79. Du L, Imgram G and Dominy RG. Time-accurate blade surface static pressure behaviour on a rotating H-Darrieus wind turbine. *Wind Energy* 2019. DOI: 10.1002/we.2307.
80. Bianchini A, Marten D, Tonini A, et al. Implementation of the "Virtual Camber" Transformation into the Open Source Software QBlade: Validation and Assessmen. *Energy Procedia* 2018; 148: 210-217.
81. Balduzzi F, Bianchini A, Maleci R, et al. Blade Design Criteria to Compensate the Flow Curvature Effects in H-Darrieus Wind Turbines. *J Turbomach* 2015; 137.

82. Staelens Y, Saeed F and Paraschivoiu I. A straight-bladed variable-pitch VAWT concept for improved power generation. *ASME 2003 Wind Energy Symposium*. Reno, Nevada, USA, 6–9 January 2003, Paper No. WIND2003-5242003.
83. Bossanyi EA. Wind turbine control for load reduction. *Wind Energy* 2003; 6: 229-244.
84. Kosaku T, Sano M and Nakatani K. Optimum pitch control for variable-pitch vertical-axis wind turbines by a single stage model on the momentum theory. *IEEE International Conference on Systems*. 2002.
85. Vandenberghe D, and Dick E. Optimum pitch control for vertical axis wind turbines. *Wind Engineering* 1987; 11: 237-247.
86. Chougule P, and Nielsen S. Overview and Design of self-acting pitch control mechanism for vertical axis wind turbine using multi body simulation approach. *J Phys Conf Ser* 2014; 524.
87. Chen B, Su S, Viola IM, et al. Numerical investigation of vertical-axis tidal turbines with sinusoidal pitching blades. *Ocean Engineering* 2018; 155: 75-87.
88. Abdalrahman G, Melek W and Lien F. Pitch angle control for a small-scale Darrieus vertical axis wind turbine with straight blades (H-Type VAWT). *Renewable Energy* 2017; 114: 1353-1362.
89. Vandenberghe D, and Dick E. A theoretical and experimental investigation into straight bladed vertical axis wind turbine with second order harmonic pitch control. *Wind Engineering* 1987; 11: 237-247.
90. Bhutta M, Hayat N, Farooq AU, et al. Vertical axis wind turbine – A review of various configurations and design techniques. *Renewable and Sustainable Energy Reviews* 2012; 16: 1926-1939.
91. Pearson C. *Vertical Axis Wind Turbine Acoustics*. PhD Thesis, Cambridge University, UK, 2013.
92. Rezaeiha A, Kalkman I and Blocken B. Effect of pitch angle on power performance and aerodynamics of a vertical axis wind turbine. *Appl Energy* 2017; 197: 132-150.
93. Parra-Santos T, Trullen DJP, Gallegos A, et al. INFLUENCE OF FIXED PITCH ANGLE ON THE PERFORMANCE OF SMALL SCALE. *Proceedings of the ASME 2016 Fluids Engineering Division Summer Meeting*. Washington, DC, USA, 10-14 July 2016.
94. Ashwill TD. *Measured Data for the Sandia 34m Vertical Axis Wind Turbine*. Sandia Laboratories, SAND91-2228, 1992.
95. Li Y, Tagawa K and Liu W. Performance effects of attachment on blade on a straight-bladed vertical axis wind turbine. *Curr Appl Phys* 2010; 10: S335-338.
96. Priegue L, and Stoesser T. The influence of blade roughness on the performance of a vertical axis tidal turbine. *International Journal of Marine Energy* 2017; 17: 136-146.
97. Edwards JM. *The Influence of Aerodynamic Stall on the Performance of Vertical Axis Wind Turbines*. PhD thesis, Sheffield University, UK, 2012.
98. Meana-Fernandez A, Solis-Gallego I, Oro JMF, et al. Parametrical evaluation of the aerodynamic performance of vertical axis wind turbines for the proposal of optimized designs. *Energy* 2018; 147: 504-517.
99. Amstrong S, Fiedler A and Tullis S. Flow separation on a high Reynolds number, high solidity vertical axis wind turbine with straight and canted blades and canted blades with fences. *Renewable Energy* 2012; 41: 13-22.
100. Zanforlin S, and Deluca S. Effects of the Reynolds number and the tip losses on the optimal aspect ratio of straight-bladed Vertical Axis Wind Turbines. *Energy* 2018; 148: 179-195.
101. Sheldahl RE, Klimas PC and Feltz LV. *Aerodynamic Performance of a 5-metre Diameter Darrieus Turbine With Extruded NACA-0015 Blades*. Sandia Laboratories, SAND80-0179, 1980.
102. Danao LA, Eboibi O and Howell R. An experimental investigation into the influence of unsteady wind on the performance of a vertical axis wind turbine. *Appl Energy* 2014; 116: 111-124.
103. Jin X, Zhao G, Gao K, et al. Darrieus vertical axis wind turbine: Basic research methods. *Renewable and Sustainable Energy Reviews* 2015; 42: 212-225.
104. Islam M, Ting DSK and Fartaj A. Aerodynamic models for Darrieus-type straight-bladed vertical axis wind turbines. *Renewable and Sustainable Energy Reviews* 2008; 12: 1087-1109.
105. Strickland JH. *The Darrieus Turbine: A Performance Prediction Model Using Multiple Streamtubes*. Sandia Laboratories, SAND75-0431, 1975.
106. Muraca RJ, Stephens MV and Dagenhart JR. *Theoretical performance of cross-wind axis turbines with results for a catenary vertical axis configuration*. NASA TMX-72662, USA, 1975.
107. Sharpe DJ. *A theoretical and experimental study of the Darrieus vertical axis wind turbine*. School of Mechanical, Aeronautical & Production Engineering. Kingston Polytechnic, 1977.
108. Read S, and Sharpe DJ. *An extended multiple streamtube theory for vertical axis wind turbines*. 1980. Cranfield, UK: 2nd BWEA workshop.
109. Tai FZ, Kang KW and Jang MH. Study on the analysis method for the vertical-axis wind turbines having Darrieus blades. *Renewable Energy* 2013; 54: 26-31.
110. Lapin EE. Theoretical performance of vertical axis wind turbines. *Proceedings of the Winter Annual Meeting*. Houston, TX, USA, 1975.

111. Paraschivoiu I. Double-Multiple Streamtube Model for Darrieus Wind Turbines. *Second DOE/NASA Wind Turbines Dynamics Workshop,* . Cleveland, USA, 1981.
112. Paraschivoiu I, Delclaux F, Fraunie P, et al. Aerodynamic analysis of the darrieus rotor including secondary effects. *Energy* 1983; 7: 416-421.
113. Saeidi D, Sedaghat A, Alamdari P, et al. Aerodynamic design and economical evaluation of site specific small vertical axis wind turbines. *Appl Energy* 2013; 101: 765-775.
114. Svorcan J, Komarov D, Peković O, et al. Aerodynamic design and analysis of a small-scale vertical axis wind turbine. *Journal of Mechanical Science and Technology* 2013; 27: 2367-2373.
115. Bianchini A, Ferrara G and Ferrari L. Design guidelines for H-Darrieus wind turbines: Optimization of the annual energy yield. *Energy Convers Manag* 2015; 89: 690-707.
116. Blusseau P, and Patel MH. Gyroscopic effects on a large vertical axis wind turbine mounted on a floating structure. *Renewable Energy* 2012; 46: 31-42.
117. Larsen HC. Summary of a vortex theory for the cyclogyro. *Proceedings of the second US national conferences on wind engineering research*. Colorado state university, 1975.
118. Wilson RE. Wind-turbine aerodynamics. *Wind Engineering and Industrial Aerodynamics* 1980: 357-372.
119. Holme OA. Contribution to the aerodynamic theory of the vertical axis wind turbine. *International symposium, on wind energy systems*.
120. Fanucci JB, and Walter RE. *Innovative wind machines: the theoretical performance of a vertical-axis wind turbine*. Sandia laboratories, SAND76-5586, 1976.
121. Strickland JH, Webster BT and Nguyen T. A Vortex model of the darrieus turbine: an analytical and experimental study. *J Fluids Eng* 1979; 101: 500-505.
122. Strickland JH, Webster BT and Nguyen T. *A Vortex Model of the Darrieus Turbine: An Analytical and Experimental Study*. Sandia Laboratories, SAND81-7017, 1981.
123. Cardona JL. Flow curvature and dynamic stall simulated with an aerodynamic freevortex model for VAWT. *Wind Engineering* 1984; 8: 135-143.
124. Pawsey NCK. *Development and Evaluation of Passive Variable-Pitch Vertical Axis Wind Turbines*. 2002.
125. Dumitrescu H. Low-frequency noise prediction of vertical axis wind turbines. *In Proceedings of the Romanian Academy, Series A* 2010; 11: 47-54.
126. Scheurich F, Fletcher TM and Brown RE. Simulating the aerodynamic performance and wake dynamics of Vertical Axis Wind Turbine. *Wind Energy* 2010; 14: 159-177.
127. Brown RE. Rotor wake modelling for flight dynamic simulation of helicopters. *AIAA J* 2000; 38: 57-63.
128. Hirsch H, and Mandal AC. A cascade theory for the aerodynamic performance of darrieus wind turbines. *Wind Engineering* 1987; 11: 164-175.
129. Mandal AC, and Burton JD. The effects of dynamic stall and flow curvature on the aerodynamics of darrieus turbines applying the Cascade model. *Wind Engineering* 1994; 18: 267-282.
130. Hand B, and Cashman A. Aerodynamic modeling methods for a large-scale vertical axis wind turbine: A comparative study. *Renewable Energy* 2018; 129: 12-31.
131. Hand B, Cashman A and Kelly G. A Low-Order Model for Offshore Floating Vertical Axis Wind Turbine Aerodynamics. *IEEE Trans Ind Appl* 2016; 14.
132. Daroczy L, Janiga G, Petrasch K, et al. Comparative analysis of turbulence models for the aerodynamic simulation of H-Darrieus rotors. *Energy* 2015: 1-11.
133. Lee Y-T, and Lim H-C. Numerical study of the aerodynamic performance of a 500 W Darrieus-type vertical-axis wind turbine. *Renewable Energy* 2015; 83: 407-415.
134. Ghasemian M, Ashrafi ZN and Sedaghat A. A review on computational fluid dynamic simulation techniques for Darrieus vertical axis wind turbines. *Energy Convers Manag* 2017; 149: 87-100.
135. McNaughton J, Billard F and Revell A. Turbulence modeling of low Reynolds number flow effects around a vertical axis turbine at a range of tip-speed ratios. *J Fluids Struct* 2014; 47: 124-138.
136. Danao LA, Edwards J, Eboibi O, et al. A numerical investigation into the influence of unsteady wind on the performance and aerodynamics of a vertical axis wind turbine. *Appl Energy* 2014; 116: 111-124.
137. Bhargav MMSRS, Kishore VR and Laxman V. Influence of fluctuating wind conditions on vertical axis wind turbine using a three dimensional CFD model. *Wind Engineering and Industrial Aerodynamics* 2016; 158: 98-108.
138. Amet E, Maître T, Pellone C, et al. 2D Numerical Simulations of Blade-Vortex Interaction in a Darrieus Turbine. *J Fluids Eng* 2009; 131.
139. Castelli MR, Monte AD, Quaresimin M, et al. Numerical evaluation of aerodynamic and inertial contributions to Darrieus wind turbine blade deformation. *Renewable Energy* 2013; 51: 101-112.
140. Almohammadi KM, Ingham DB, Ma L, et al. Modeling dynamic stall of a straight blade vertical axis wind turbine. *J Fluids Struct* 2015; 57: 144-158.

141. Balduzzi F, Drofelnik J, Bianchini A, et al. Darrieus wind turbine blade unsteady aerodynamics: a threedimensional Navier-Stokes CFD assessment. *Energy* 2017; 128: 550-563.
142. Rezaeiha A, Kalkman I and Blocken B. CFD simulation of a vertical axis wind turbine operating at a moderate tip speed ratio: Guidelines for minimum domain size and azimuthal increment. *Renewable Energy* 2017; 107: 373-385.
143. Rezaeiha A, Montazeri H and Blocken B. Characterization of aerodynamic performance of vertical axis wind turbines: Impact of operational parameters. *Energy Convers Manag* 2018; 169: 45-77.
144. Wekesa DW, Wang C, Wei Y, et al. Analytical and numerical investigation of unsteady wind for enhanced energy capture in a fluctuating free-stream. *Energy* 2017; 121: 854-864.
145. Lam HF, and Peng HY. Study of wake characteristics of a vertical axis wind turbine by two- and three-dimensional computational fluid dynamics simulations. *Renewable Energy* 2016; 90: 386-398.
146. Mclaren K, Tullis S and Ziada S. Computational fluid dynamics simulation of the aerodynamics of a high solidity, small-scale vertical axis wind turbine. *Wind Energy* 2012; 15: 349-361.
147. Li C, Zhu S, Xu Y, et al. 2.5D large eddy simulation of vertical axis wind turbine in consideration of high angle of attack flow. *Renewable Energy* 2013; 51: 317-330.
148. Elkhoury M, Kiwata T and Aoun E. Experimental and numerical investigation of a three-dimensional vertical-axis wind turbine with variable-pitch. *Wind Engineering and Industrial Aerodynamics* 2015; 139: 111-123.
149. Patil R, Daroczy L, Janiga G, et al. Large eddy simulation of an H-Darrieus rotor. *Energy* 2018; 160: 388-398.
150. Peng HY, and Lam HF. Turbulence effects on the wake characteristics and aerodynamic performance of a straight-bladed vertical axis wind turbine by wind tunnel tests and large eddy simulations. *Energy* 2016; 109: 557-568.
151. Ghasemian M, and Nejat A. Aero-acoustics prediction of a vertical axis wind turbine using Large Eddy Simulation and acoustic analogy. *Energy* 2015; 88: 711-717.
152. Lei H, Zhou D, Bao Y, et al. Three-dimensional Improved Delayed Detached Eddy Simulation of a two-bladed vertical axis wind turbine. *Energy Convers Manag* 2017; 133: 235-248.
153. Rezaeiha A, Montazeri H and Blocken B. Towards accurate CFD simulations of vertical axis wind turbines at different tip speed ratios and solidities: Guidelines for azimuthal increment, domain size and convergence. *Energy Convers Manag* 2018; 156: 301-316.
154. Mankowski O-A. *The Wind Tunnel Simulation and Effect of Turbulent Air flow on Automotive Aerodynamics*. PhD Thesis, Unverisity of Durham, UK, 2013.
155. Mazarbhuiya H, Biswas A and Sharma KK. Performance investigations of modified asymmetric blade H-Darrieus VAWT rotors. *Renewable and Sustainable Energy* 2018; 10.
156. Weber J, Becker S, Scheit C, et al. Aeroacoustics of Darrieus wind turbine. *Aeroacoustics* 2015; 14: 883-902.
157. Molina AC, Massai T, Balduzzi F, et al. Combined experimental and numerical study on the near wake of a Darrieus VAWT under turbulent flows. *J Phys Conf Ser* 2018.
158. Bianchini A, Balduzzi F, Ferrara G, et al. Detailed Analysis of the Wake Structure of a Straight-Blade H-Darrieus Wind Turbine by Means of Wind Tunnel Experiments and Computational Fluid Dynamics Simulations. *J Eng Gas Turbine Power* 2018; 140.
159. Greenblatt D, Schulman M and Ben-Harav A. Vertical axis wind turbine performance enhancement using plasma actuators. *Renewable Energy* 2012; 37: 345-354.
160. Peng HY, Lam HF and Lee CF. Investigation into the wake aerodynamics of a five-straight-bladed vertical axis wind turbine by wind tunneltests. *Wind Engineering and Industrial Aerodynamics* 2016; 155: 23-35.
161. Elkhoury M, Kiwata T, Nagao K, et al. Wind tunnel experiments and Delayed Detached Eddy Simulation of a three-bladed micro vertical axis wind turbine. *Renewable Energy* 2018; 129: 63-74.
162. Battist L, Brighenti A, Castelli MR, et al. Performance and midspan wake measurements on a H-Darrieus in controlled conditions. *J Phys Conf Ser* 2018; 1037: 022041.
163. Chong WT, Fazlizan A, Poh SC, et al. The design, simulation and testing of an urban vertical axis wind turbine with the omni-direction-guide-vane. *Appl Energy* 2013; 112: 601-609.
164. Li Q, Maeda T, Kamada Y, et al. Wind tunnel and numerical study of a straight-bladed Vertical AxisWind Turbine in three-dimensional analysis (Part II: For predictingflow field and performance). *Energy* 2016; 104: 295-307.
165. Du L, Imgram G and Dominy RG. Experimental study of the effects of turbine solidity, blade profile, pitch angle, surface roughness, and aspect ratio on the H‐Darrieus wind turbine self-starting and overall performance. *Energy Sci Eng* 2019; 0: 1-16. DOI: 10.1002/ese3.430.
166. Fujisawa N, and Shibuya S. Observations of dynamic stall on Darrieus wind turbine blades. *Wind Engineering and Industrial Aerodynamics* 2001; 89: 201-214.

167. Posa A, Parker CM, Leftwich MC, et al. Wake structure of a single vertical axis wind turbine. *Int J Heat Fluid Flow* 2016; 61: 75-84.
168. Ferreira CS, Kuik GV, Bussel GV, et al. Visualization by PIV of dynamic stall on a vertical axis wind turbine. *Exp Fluids* 2009; 46: 97-108.
169. Tescione G, Ragni D, He K, et al. Near wake flow analysis of a vertical axis wind turbine by stereoscopic particle image velocimetry [J]. *Renewable Energy* 2014; 70: 47-61.
170. Rolin VF-C, and Porte-Agel F. Experimental investigation of vertical-axis wind-turbine wakes in boundary layer flow. *Renewable Energy* 2018; 118: 1-13.
171. Buchner AJ, Lohry MW, Martinelli L, et al. Dynamic stall in vertical axis wind turbines: Comparing experiments and computations. *Wind Engineering and Industrial Aerodynamics* 2015; 146: 163-171.
172. Rolland SA, Thatcher M, Ellis R, et al. Performance assessment of a vertical axis turbine in a marine current flume tank and CFD modelling. *International Journal of Marine Energy* 2015; 12: 35-45.
173. Hohman TC, Martinelli L and Smits AJ. The effects of inflow conditions on vertical axis wind turbine wake structure and performance. *Wind Engineering and Industrial Aerodynamics* 2018; 183: 1-18.
174. Ouro P, Runge S, Luo Q, et al. Three-dimensionality of the wake recovery behind a vertical axis turbine. *Renewable Energy* 2018; 133: 1066-1077.
175. Maeda T KY, Murata J, et al. . Measurements of flow field and pressure distribution of straight-bladed vertical axis wind turbine. *Proceedings of European wind energy association conference and exhibition 2013; Vienna, Austria; February 4–6* 2013.
176. Li Q MT, Kamada Y, et al. Measurement of the flow field around straight-bladed vertical axis wind turbine. *Wind Engineering and Industrial Aerodynamics* 2016; 151: 70-78.
177. Ryan KJ, Coletti F, Elkins CJ, et al. Three-dimensional flow field around and downstream of a subscale model rotating vertical axis wind turbine. *Exp Fluids* 2016; 57.
178. Li Q, Maeda T, Kamada Y, et al. Wind tunnel and numerical study of a straight-bladed vertical axis wind turbine in three-dimensional analysis (Part I: For predicting aerodynamic loads and performance). *Energy* 2016; 106: 443-452.
179. Sims-Williams D. Self-excited Aerodynamic Unsteadiness Associated with Passenger Cars. *Dissertation, Unverisity of Durham, UK* 2001.
180. Sims-Williams D, Luck DA. Transfer function characterization of pressure signal tubes for the measurement of large amplitude pressure fluctuations. *Proceedings of the Institution of Mechanical Engineers, Part C: Journal of Mechanical Engineering Science* 2007; 221: 707-771.